TEMPORARILY ALLOYING TITANIUM TO FACILITATE FRICTION STIR WELDING

By

YURI HOVANSKI

A thesis submitted in partial fulfillment of
the requirements for the degree of

MASTER OF SCIENCE IN MECHANICAL ENGINEERING

WASHINGTON STATE UNIVERSITY
Department of Mechanical Engineering

May 2009

To the Faculty of Washington State University:

The members of the Committee appointed to examine the thesis of YURI HOVANSKI find it satisfactory and recommend that it be accepted.

_____
William C. Kinsel, Ph.D., Chair

_____
David P. Field, Ph.D.

_____
Hussein M. Zbib, Ph.D.

ACKNOWLEDGMENT

The author wishes to gratefully acknowledge the financial assistance of a Laboratory Directed Research and Development project from Battelle – Pacific Northwest Division as well as the continued financial support of Dr. Joseph Carpenter via the Automotive Lightweight Materials program. All research herein was performed at the campus of the Pacific Northwest National Laboratory. Gratitude is also expressed for the technical support of Mr. Stan Pitman who assisted in the development of the thermohydrogen processing parameters as well as for the expertise and advice of Mr. Curt A. Lavender and Dr. K. Scott Weil who spent countless hours advising Mr. Hovanski in the intricacies of titanium and titanium metallurgy.

TEMPORARILY ALLOYING TITANIUM TO FACILITATE

FRICTION STIR WELDING

ABSTRACT

by Yuri Hovanski, M.S.
Washington State University
May 2009

Chair: William C. Kinsel

While historically hydrogen has been considered an impurity in titanium, when used as a temporary alloying agent it promotes beneficial changes to material properties that increase the hot-workability of the metal. This technique known as thermohydrogen processing was used to temporarily alloy hydrogen with commercially pure titanium sheet as a means of facilitating the friction stir welding process. Specific alloying parameters were developed to increase the overall hydrogen content of the titanium sheet ranging from commercially pure to 30 atomic percent. Each sheet was evaluated to determine the effect of the hydrogen content on process loads and tool deformation during the plunge phase of the friction stir welding process. Two materials, H-13 tool steel and pure tungsten, were used to fabricate friction stir welding tools that were plunged into each of the thermohydrogen processed titanium sheets. Tool wear was characterized and variations in machine loads were quantified for each tool material and weld metal combination.

Thermohydrogen processing was shown to beneficially lower plunge forces and stabilize machine torques at specific hydrogen concentrations. The resulting effects of hydrogen addition to titanium metal undergoing the friction stir welding process are compared with modifications in titanium properties documented in modern literature.

Such comparative analysis is used to explain the variance in resulting process loads as a function of the initial hydrogen concentration of the titanium.

TABLE OF CONTENTS

Page

ACKNOWLEDGMENT iii

ABSTRACT iv

LIST OF TABLES vii

LIST OF FIGURES viii

NOMENCLATURE ix

CHAPTER

1. INTRODUCTION 1
   - Thermohydrogen Processing 4
   - Friction Stir Welding Titanium Alloys 7

2. DESIGN PARAMETERS AND TEST CONFIGURATION 10
   - Controlled Alloying of Titanium Sheet with Hydrogen 10
   - Tool Design and Material Selection 12
   - Friction Stir Welding Plunge Testing 13

3. ANALYSIS AND DISCUSSION OF RESULTS 18
   - Controlled Alloying of Titanium Sheet with Hydrogen 18
   - Tool Performance 21
   - Friction Stir Welding Plunge Testing 23
   - Effect of Hydrogen on Flow Stress in Commercially Pure Titanium 27

4. CONCLUSIONS AND FUTURE RECOMMENDATIONS 33
   - Future Recommendations 34

5. BIBLIOGRAPHY 35

6. APPENDIX 39
   - Appendix A: FSW Tool Drawing 39
   - Appendix B: Molar Breakdown of Hydrogen Content 40
   - Appendix C: Reaction Forces and Torques Using an H-13 Tool 41
   - Appendix D: Reaction Forces and Torques Using a Tungsten Tool 44

LIST OF TABLES

Table 1. Plunge test schedule. 16

Table 2. Specimen weight targets and actual weights used to determine hydrogen content in thermohydrogen processed commercially pure titanium sheet 19

Table 3. Tabulated values of average peak loads and average peak torques recorded during FSW plunge tests in thermohydrogen processed commercially pure titanium sheets. 27

LIST OF FIGURES

Figure 1. Schematic illustration of FSW process..... 1

Figure 2. Binary phase diagram for the titanium-hydrogen system at or below 1 MPa. ... 6

Figure 3. Detailed drawing of the friction stir welding tool pin used for plunge testing in thermohydrogen processed titanium. 12

Figure 4. High stiffness friction stir welding machine located at the Pacific Northwest National Laboratory in Richland Washington. 13

Figure 5. Friction stir welding tool loaded into a #50 collet chuck tool holder. 14

Figure 6. Schematic layout of plunge tests, showing the minimum 50 mm (2 inch) spacing between plunge locations on the titanium sheet. 17

Figure 7. Stress-Strain curve of dehydrided commercially pure titanium sheet. Yield Stress of more than 400 MPa with a 48% area reduction. 20

Figure 8. As-tested tensile specimens of dehydrided commercially pure titanium. 21

Figure 9. Material buildup on tungsten tools after three FSW plunge tests in CP-Ti alloyed with 10 (left), 20 (middle) and 30 (right) atomic percent hydrogen. 22

Figure 10. Tool reaction loads showing the increased data scatter for hydrogen contents above 10 atomic percent. 25

Figure 11. H-13 friction stir welding tool after three plunges in titanium sheet alloyed with 20% atomic hydrogen. 26

Figure 12. Load and torque magnitudes for a FSW plunge test using a tungsten tool in commercially pure titanium sheet. 29

Figure 13. Load and torque magnitudes for a FSW plunge test using a tungsten tool in titanium sheet alloyed to 10% atomic hydrogen. 30

Figure 14. Load and torque magnitudes for a FSW plunge test using an H-13 tool in commercially pure titanium sheet. 31

Figure 15. Load and torque magnitudes for a FSW plunge test using an H-13 tool in titanium sheet alloyed to 5% atomic hydrogen. 32

NOMENCLATURE

PNNL	Pacific Northwest National Laboratory
WSU	Washington State University
FSW	Friction Stir Welding
CP-Ti	Commercially Pure Titanium
THP	Thermohydrogen Processing
DARPA	Defense Advanced Research Projects Agency
hcp	Hexagonal close pack
bcc	Body-centered cubic
°C	Degrees Celsius
At.%	Atomic percent
Al	Aluminum
V	Vanadium
RPM	Rotations per minute
mm	Millimeters
sccm	Standard cubic centimeters per minute
MPa	Megapascals
α	Alpha phase titanium
β	Beta phase titanium
α + β	Alpha-beta mixed phase
PCBN	Poly-crystalline cubic boron nitride

Dedication

This thesis is primarily dedicated to my loving wife Candice.
Her unwavering support and love helped me to stay on track and finish what I started.

I also dedicate this work to my father and other mentors and professors who diligently worked to instill in me a love of mechanisms, science, materials and engineering.

Thank you.

CHAPTER ONE

INTRODUCTION

Friction Stir Welding (FSW) is a relatively new solid state joining process that has found wide spread acceptance throughout the welding and joining community since its inception in 1991 by The Welding Institute [1]. The process employs a non-consumable cylindrical tool that is rotated and plunged into the interface of two materials and subsequently translated down that interface to form a linear weld. A schematic illustration of the process in a butt weld configuration is shown in Figure 1. Distinctive nomenclature associated with the process has been labeled within the Figure below, showing the differences between advancing, retreating, leading and trailing locations in the weld.

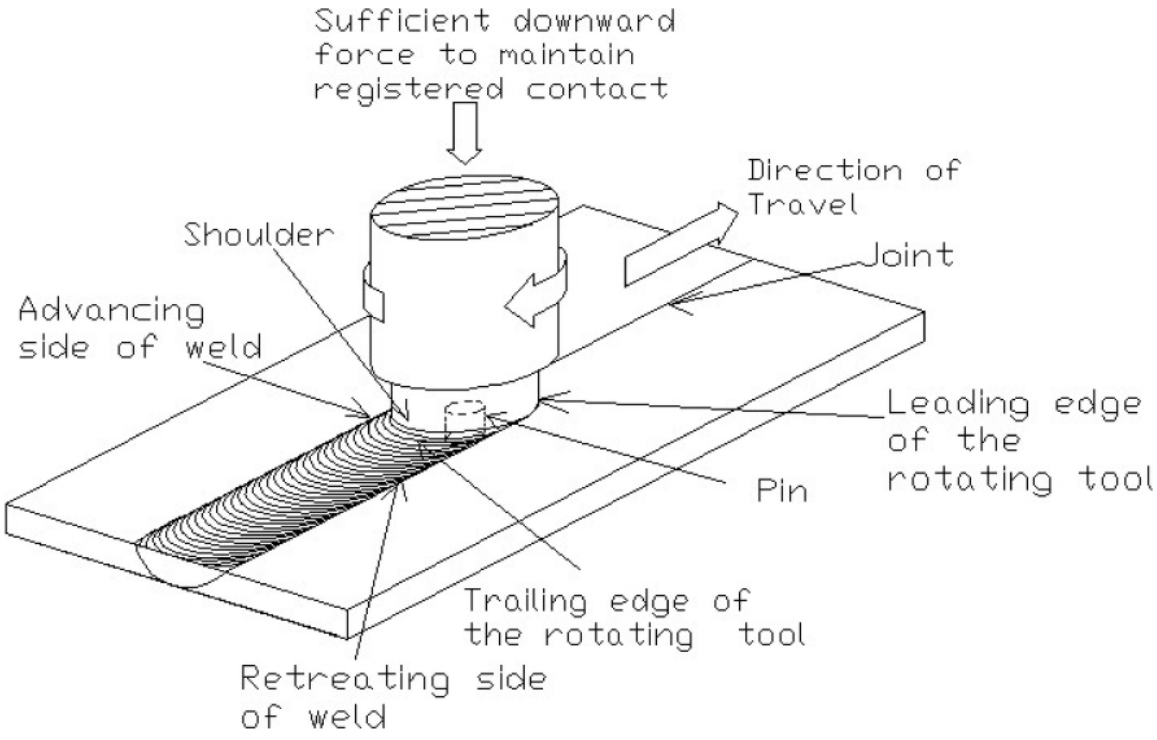

Figure 1. Schematic illustration of FSW process.

Applications for FSW in light weight materials such as aluminum became immediately apparent as the rapid implementation of low-cost, emission free FSW quickly overcame the historical difficulties of welding aluminum alloys [2-4]. Implementation of FSW in higher strength materials such as steel and titanium is proving more problematic, for traditional fusion welding and solid state joining techniques such as diffusion bonding are already industrially acceptable for these high strength materials. Thus, the justification for implementing FSW in such material systems was developed more as a means of enhancing the processability and properties of joints than as a competing joining technology. Such is the case with FSW titanium structures, where specific processing parameters can be developed to provide refined grain structures within the welded region closely resembling the parent material. Such Microstructural modification allows for retention of crucial properties such as uniform formability, corrosion resistance, and other mechanical properties that originally led to the selection of a titanium alloy.

FSW of titanium alloys has recently received a great deal of attention leading to a sizable Defense Advanced Research Projects Agency (DARPA) program to enable the process as part of a larger more comprehensive titanium initiative [5]. This program and other more independent research investigations have shown marked progress in the successful joining of titanium alloys via FSW [6-10]. However, while significant research and development has specifically focused on the selection of appropriate tool materials for FSW titanium alloys, industrial deployment of this technology is still hampered by an inability to provide high-cycle, reusable tooling that is readily accessible and cost efficient [6-7, and 11].

Tool failures in titanium alloys are primarily related to excessive wear and deformation that occur during the initial plunge phase of the FSW process, in which the rotating tool is thrust into the weld material [6-8]. Deformation of the tool pin, the reduced diameter section of the tool beneath the larger tool shoulder, generally yields a reduction in the pin length that result in insufficient weld depth to consolidate the lower regions of the weld joint. This problem is further exacerbated by the chemical reactivity of titanium with many carbon based superabrasives that prevents the use of typical materials used for friction stir welding high strength materials.

Investigations up to this point have focused on finding the proper tool material to survive the heat, friction, reaction forces and chemical reactivity inherent in FSW titanium alloys; however, little has been done to investigate the potential of temporarily modifying the material to facilitate the FSW process. Historically the interaction of hydrogen and titanium has been strictly avoided in production and processing of titanium alloys, yet increased understanding of the unique alloying properties of hydrogen in titanium are being further explored. Modern research shows that hydrogen utilized as a temporary alloying element in titanium alloys provides enhancements in areas such as hot workability, machining, sintering and compaction while simultaneously providing for controlled modification of specific mechanical properties including ultimate and yield stress, bulk and shear modulus, and elongation [12-18]. The data amassed relating the beneficial nature of such temporary alloying, known as Thermohydrogen Processing, has yet to find wide spread utilization due to numerous factors including the strict aerospace regulations prohibiting hydrogen contamination in titanium alloys. Nevertheless, distinct

areas show that small scale deployment of thermohydrogen processing is enabling processing and production of titanium that were previously untouched [19-27].

Commercially pure titanium sheet was temporarily alloyed with hydrogen to facilitate FSW by selectively modifying the material properties to reduce process loads and deter chemical reactivity. Thermohydrogen processing conditions were developed to alloy titanium with hydrogen at varied mixture ratios ranging from commercially pure to thirty atomic percent hydrogen.

As tool failure in titanium FSW is generally related to deformation of the pin during the plunge phase, extensive linear testing was determined to be out of the scope of this study. As such, numerous plunge tests were conducted on each of the thermohydrogen processed titanium sheets. Loads and torques were monitored and recorded during these plunge experiments, and were systematically compared to evaluate the influence of varied hydrogen concentrations on process loads during the plunge phase of the FSW process. Tool wear and reactivity were also characterized in order to determine the effective lifecycle of each tool material combination.

Thermohydrogen Processing

The use of hydrogen as a temporary alloying element to improve the processing, microstructure, and mechanical properties of titanium alloys has become known as thermohydrogen processing [20-21, 23, and 25-26]. This process entails adding hydrogen to a titanium alloy by exposing the material to a hydrogen environment at an increased temperature, performing a subsequent heat treatment or thermomechanical processing, and finally removing the hydrogen via a vacuum anneal. The practice of

modifying the properties of titanium metals with hydrogen alloying is based on the influence of hydrogen on the kinetics of phase transformations, the overall phase compositions, and the ability to form novel metastable phases. Such metallurgical changes provide a number of advantages when processing titanium alloys including increased hot workability of the α, pseudo-α and α + β phases [20-21, and 24-27].

Examination of the binary phase diagram for the titanium-hydrogen system, Figure 2, shows that an addition of a small percentage of hydrogen quickly destabilizes the low temperature hcp α-phase allowing some portion of the α-phase to be transformed into the bcc β-phase. Consequently an addition of hydrogen also stabilizes the higher temperature bcc β-phase by lowering the temperature of the α to β phase transformation. Furthermore, an initial increase in hydrogen further promotes the two-phase (α + β) region above approximately 7 % atomic at the eutectoid temperature. These fundamental differences in the phase kinetics of titanium metal lead to changes in the rate and temperature of martensite transformations, with increasing hydrogen concentrations yielding reductions in both the temperature of formation and rate of cooling required to induce such transformations. Such basic alterations in the structure and phase kinetics of the material are consequential due to the significant reduction or inflation of material properties specific to each phase in the titanium-hydrogen system. An example of the effect of such distinct changes in the material properties from phase to phase is the rapid decrease in the shear and Young's moduli of the α phase with increasing hydrogen content. In contrast, a similar increase in the hydrogen content of the β-phase leads to an increase in both moduli [12-13].

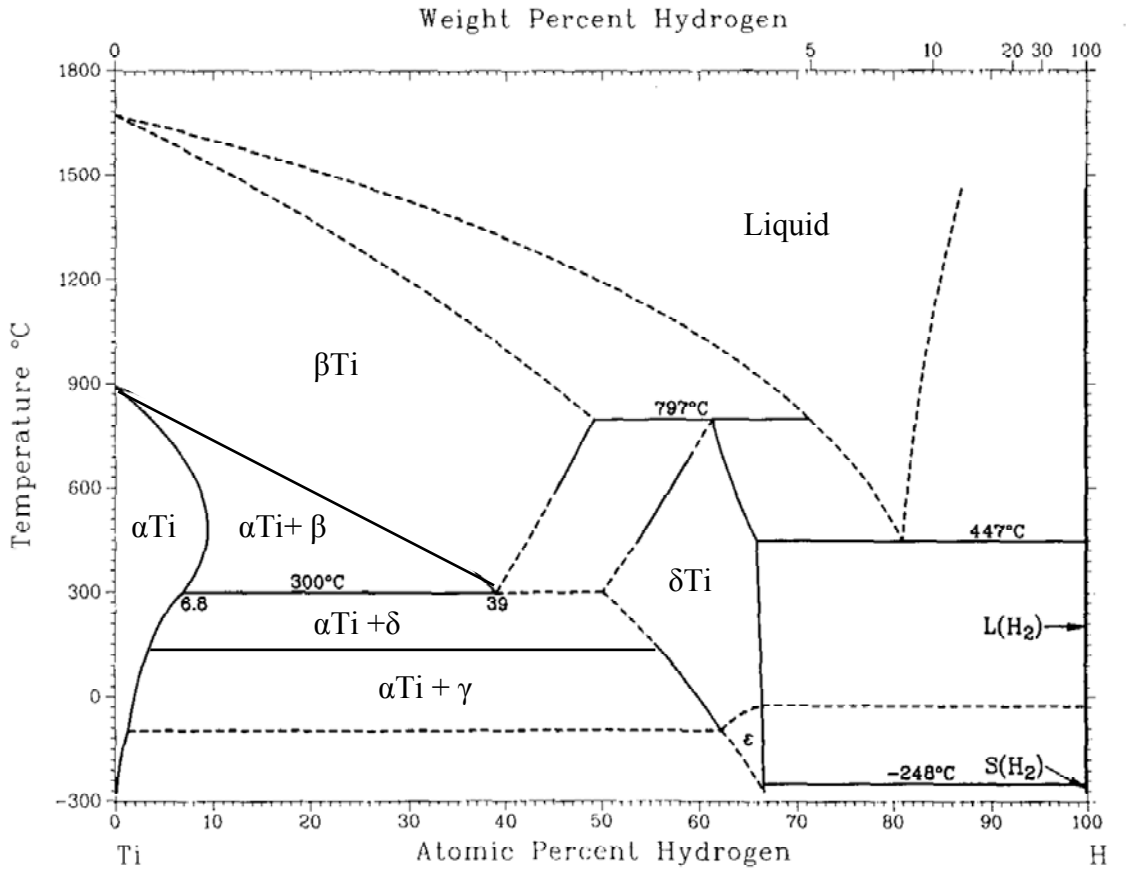

Figure 2. Binary phase diagram for the titanium-hydrogen system at or below 1 MPa.

Figure 2 demonstrates that an addition of roughly 39 at.% hydrogen reduces the α to β phase transformation temperature from 882°C to 300°C. This nearly linear relationship shows that an increase of one atomic percent hydrogen yields a reduction of approximately 13.7°C in the beta transus temperature. As the β phase shows no stability below the eutectoid temperature, a combination of α + δ phase are formed for hydrogen concentrations above 6.8% atomic and below 300°C followed by a transformation to an α + γ phase below 168°C. These subsequent cooling transformations lead to volumetric

expansion that develop considerable internal stresses often manifesting themselves in visible distortion of the hydrogen alloyed metal as reported by others [40-42]

Thermohydrogen processing of titanium alloys is often used to stabilize the β phase by adding sufficient hydrogen to prevent phase changes during processing. Such phase stabilization during processing can prevent catastrophic failures during forming and joining that are created from the significant and rapid changes in material properties that take place at the transition between the α and β phases. Thus, stabilization of either phase simply allows for more uniform performance without sudden shifts in reaction loads from the titanium metal. As many hot working processes take place at or near the β-transus of commercially pure titanium, thermohydrogen processing provides a means of stabilizing the β phase by effectively lowering the transition temperature below the effective operation condition. Many of the variations of thermohydrogen processing techniques were previously summarized [20-21, and 25-26].

Friction Stir Welding Titanium Alloys

The commencement of FSW in aluminum alloys in the early nineties stemmed a flurry of activity applying this technology to other material systems. FSW provides many advantages joining aluminum alloys when compared to traditional fusion welding including elimination of toxic cover gases, reduced power consumption, increased repeatability and safety as well as numerous positive benefits in the post-weld microstructure that enhance the final mechanical properties. To date, FSW has been commercially developed for numerous aluminum alloys, and has been demonstrated in copper, magnesium, zinc, mild and advanced high strength steel alloys, stainless steels,

polymers, cast iron, titanium alloys and dissimilar combinations of the same [33]. While FSW of aluminum and other low melting, structural alloys has rapidly matured and found widespread industrial utilization, further development is required for higher temperature materials like titanium and steels.

Attempts at FSW titanium alloys were first reported in the late nineteen nineties, and have since been made in numerous titanium alloys over the past decade, including commercially pure titanium, titanium 6Al-4V and other alpha-beta alloys, near alpha alloys, and beta alloys [6, 8, and 10]. Results varied from complete tool failure to the production of commercially viable joints with remarkable post-weld properties

While commercial success in aluminum alloys is unfettered, numerous advances are yet required to enable wide spread applicability of friction stir joining in higher strength material systems. One such advancement was the application of polycrystalline cubic boron nitride (PCBN) and other super abrasive resistant materials in FSW tool manufacturing that have greatly enabled this joining process in steels. Unfortunately, these same tool materials cannot be used in titanium alloys due to the increased affinity of titanium to react with key elements within PCBN. Attempts to use tooling manufactured from PCBN and super abrasive materials have often proven disastrous on the first plunge, with costly tooling being effectively eroded and chemically etched away in seconds.

Significant improvements have nevertheless been made in FSW titanium alloys, yet nearly all progress indicates that further evolution in tool design and materials remain the largest issue in the overall process development. Certain tungsten based materials have proven most successful, although tool wear was previously reported [6-7], and tool

deformation during the plunge phase was specifically characterized [6]. Deformation of the tool pin during the plunge phase, known as “mushrooming”, results from a combination of high reaction loads and low temperatures of the weld material during the initial tool plunge. This brief destructive period in the overall process has been somewhat mitigated as a result of state-of-the-art FSW machines that allow for variation in rotational velocities during the plunge and traverse portions of the FSW process. Results from such variation in rotational speeds were reported by Jones and Loftus [6] showing that tool deformation in a lanthanated tungsten alloy could be reduced by 50% by increasing the rotational speed during the plunge phase from 500 RPM to 900 RPM. However, even with such process modifications tool deformation during plunging remained a constant barrier preventing otherwise reusable tooling.

CHAPTER TWO

DESIGN PARAMETERS AND TEST CONFIGURATION

The objective of this study was to evaluate the effect of adding various hydrogen concentrations to commercially pure titanium on the reaction loads during the plunge phase of the FSW process. This overall objective was broken into two tasks. The first was developing a controlled alloying process for large titanium sheets, and the second was evaluating the effect of such thermohydrogen processing on the reaction loads during the plunge phase of FSW.

Controlled Alloying of Titanium Sheet with Hydrogen

Rectangular sheet specimens 137 mm in width and 406 mm in length were prepared by shearing a larger 2.54 mm thick commercially pure titanium sheet into five sections. The individual sections were subsequently alloyed with hydrogen to achieve concentrations ranging between commercially pure and 30 atomic percent hydrogen. Each sheet was individually wrapped in titanium foil as a means of gettering impurities during the alloying process. These impurities, inherent to the high purity hydrogen gas that was used as the hydrogen source during the alloying process and those present from reactions within the vacuum furnace, could otherwise inhibit the hydriding process. Specimens were placed in a vacuum furnace that was evacuated to a level of approximately 10^{-5} torr and heated to 800°C. After heating, high purity hydrogen gas was introduced to the vacuum chamber and specimen using a mass flow controller at a

rate of 200 sccm. The foil wrapped sheets were held at temperature to allow for the favorable reaction kinetics at 800°C [28-32 and 34-39] to more rapidly diffuse the hydrogen throughout the intended titanium specimen. Once the reaction was sufficiently underway, as characterized by a drop in pressure of the chamber after the introduction of the target mass of hydrogen, the temperature was lowered and held at 350°C until the balance of the reaction was complete.

The hydrogen content of each sheet was varied by controlling the mass of the hydrogen gas introduced into the vacuum chamber. The target hydrogen levels chosen for this study were commercially pure, 5, 10, 20, and 30 atomic percent. Verification of hydrogen accumulation was comparatively evaluated by measuring the difference between the initial and final mass of each specimen; each sheet was measured to the nearest 0.01 grams. Specimens were again weighed after alloying in both the wrapped and unwrapped conditions to verify the hydrogen content of both the wrapped composite and individual specimens.

Mechanical properties of the baseline titanium were initially verified via a mechanical testing and found to be essentially identical to material that had undergone thermohydrogen processing followed by subsequent vacuum annealing process to remove the hydrogen. Properties of yield strength, ultimate strength and elongation of titanium samples before and after thermohydrogen processing demonstrated little measurable deviation in samples tested in this study.

Tool Design and Material Selection

FSW tools were designed for testing thermohydrogen processed titanium sheet. Tool materials consisted of pure tungsten and H-13 hot-worked steel. Each tool was fabricated with a 1.65 mm pin length and a maximum shoulder diameter of 12.7 mm. A design drawing for the tools used in this study is presented in Appendix A, while a detailed blowup of the tool pin is shown in Figure 3. The tool was intended to provide approximately a 2:3 aspect ratio of pin to shoulder diameter at the location where the pin connects to the tool shoulder. From this location the pin diameter reduced linearly over the 1.65 mm length to a final diameter of 6.3 mm for a 1:2 aspect ratio of pin to shoulder diameter. While this tool pin is considerably wider than more traditional FSW pin tools, recent research in FSW of titanium has demonstrated their effectiveness [6-7, and 11].

H-13 tools were heat treated to H-925 after machining, and each were tested and found to have attained a hardness of 40 Rockwell C. Tungsten material utilized for tool fabrication was recrystallized rod that ranged between 37 and 39 Rockwell C at room temperature. All tungsten tools were used in their as-machined state with no coatings or heat treatment employed.

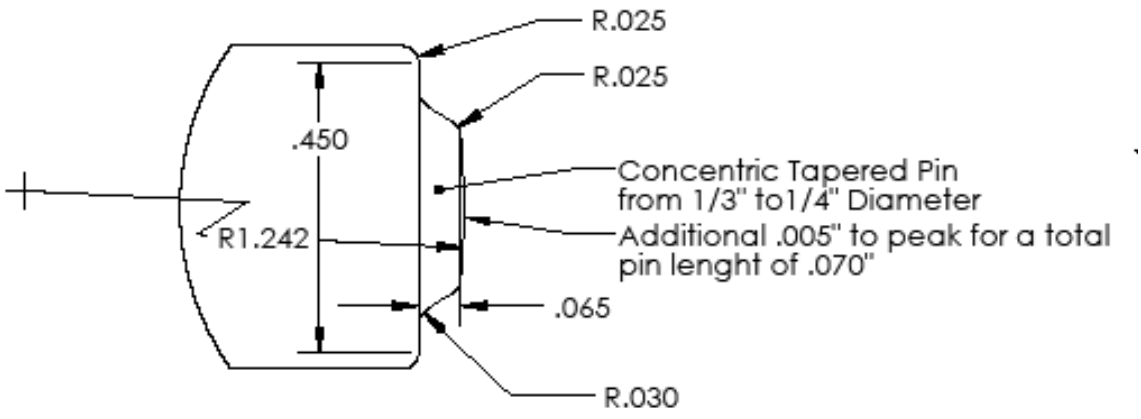

Figure 3. Detailed drawing of the friction stir welding tool pin used for plunge testing in thermohydrogen processed titanium.

Friction Stir Welding Plunge Testing

Plunge tests were designed to provide comparisons between the tool loads generated during the plunge phase of the FSW process. For plunge testing, tools were rotated and plunged (z-axis movement) into the titanium sheet, without any x-axis or y-axis translation. Initial tests were used to evaluate the effect of varying levels of hydrogen in otherwise commercially pure titanium sheet on the plunge force and torque. As a means of further characterizing the influence of hydrogen on FSW of titanium, two distinctly different tool materials were used, and each tool was plunged with identical parameters a total of three times. Tools were removed from the tool holder following each plunge, examined visually, and allowed to cool prior to further testing. A minimum spacing between plunge tests was established at roughly 50 mm to avoid any overlapping of the heat affected areas of each test case.

Figure 4. High stiffness friction stir welding machine located at the Pacific Northwest National Laboratory in Richland Washington.

All testing was performed on a Transformation Technologies Inc. friction stir welding machine located at the Pacific Northwest National Laboratory shown in Figure 4. Each sheet was clamped onto a flat, steel anvil prior to testing regardless of the distortion resulting from the alloying process. Tools were fixed into a #50 tapered collet chuck using a 9.525 mm (3/8 inch) diameter collet, allowing for tools to be shoulder loaded onto the collet face as shown in Figure 5. Neither the tools nor the tool holder were cooled during testing. To minimize oxidation of the titanium surface and tool materials an argon cover gas was constantly applied to the tool from a time prior to tool insertion until the tool had been removed for several seconds. Argon gas was applied using a copper tubing gas diffuser that liberally applied argon at a rate 14,000 sccm throughout the testing process.

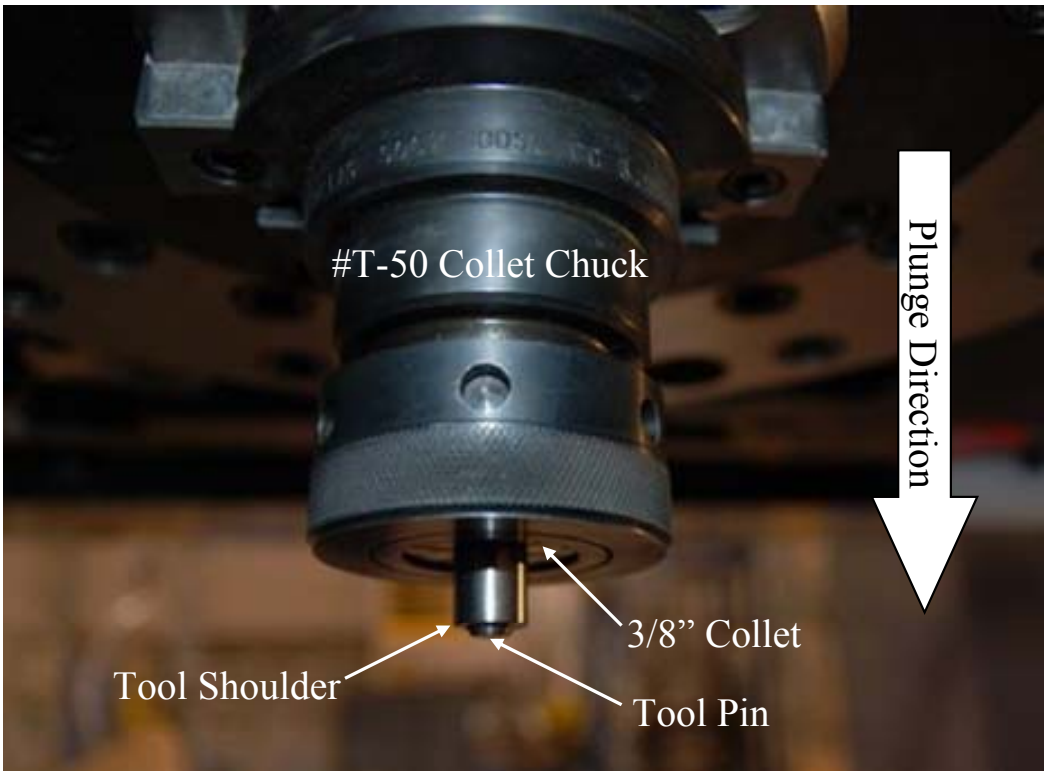

Figure 5. Friction stir welding tool loaded into a #50 collet chuck tool holder.

The data acquisitions systems on the aforementioned FSW machine provided continuous feedback of all parameters required to monitor position and load. The machine axes with respect to the tool are such that the Z-Axis aligns with the plunge direction of the tool as shown in Figure 5, the X-Axis aligns with the travel direction of a weld, and the Y-Axis is the lateral direction to the weld.

Forces and positions are monitored for each axis providing a continuous record of the commanded position or force as well as the actual or achieved value. Data acquired during plunge testing included all tool loads, machine torques, plunge depths, and machine velocities. Forces were measured by a combination of three load cells located at a fixed diameter off the z-axis (plunge axis) and separated at 120 degree intervals. Z-loads were computed as a direct summation of the resulting three magnitudes, while x-axis and y-axis forces are computed based on the moment-force relationship specific to the tool setup. Torque measurements are derived from the load variations from cell to cell, but were also directly computed from the motor drive output on the spindle motor. All position data was directly read from the motor encoders on the ball screw driven drive train.

Table 1. Plunge test schedule.

				Tool Identification			Plunge Parameters	
Plate ID	Test #	Plunge ID#	At % H	Tool ID #	Tool Material	Plunge #	Plunge Rate	Plunge RPM
CP-Ti Sheet	1	CP-1	0	H13-1	H13	1	5mm/min	400
	2	CP-2	0	H13-1	H13	2	5mm/min	400
	3	CP-3	0	H13-1	H13	3	5mm/min	400
	7	CP-7	0	W-1	W	1	5mm/min	400
	8	CP-8	0	W-1	W	2	5mm/min	400
	9	CP-9	0	W-1	W	3	5mm/min	400
Plate #2	13	H20-1	20	H13-2	H13	1	5mm/min	400
	14	H20-2	20	H13-2	H13	2	5mm/min	400
	15	H20-3	20	H13-2	H13	3	5mm/min	400
	19	H20-7	20	W-2	W	1	5mm/min	400
	20	H20-8	20	W-2	W	2	5mm/min	400
	21	H20-9	20	W-2	W	3	5mm/min	400
Plate #1	25	H10-1	10	H13-3	H13	1	5mm/min	400
	26	H10-2	10	H13-3	H13	2	5mm/min	400
	27	H10-3	10	H13-3	H13	3	5mm/min	400
	31	H10-7	10	W-3	W	1	5mm/min	400
	32	H10-8	10	W-3	W	2	5mm/min	400
	33	H10-9	10	W-3	W	3	5mm/min	400
Plate #3	37	H5-1	5	H13-4	H13	1	5mm/min	400
	38	H5-2	5	H13-4	H13	2	5mm/min	400
	39	H5-3	5	H13-4	H13	3	5mm/min	400
	43	H5-7	5	W-4	W	1	5mm/min	400
	44	H5-8	5	W-4	W	2	5mm/min	400
	45	H5-9	5	W-4	W	3	5mm/min	400
Plate #4	49	H30-1	30	H13-5	H13	1	5mm/min	400
	50	H30-2	30	H13-5	H13	2	5mm/min	400
	51	H30-3	30	H13-5	H13	3	5mm/min	400
	55	H30-7	30	W-5	W	1	5mm/min	400
	56	H30-8	30	W-5	W	2	5mm/min	400
	57	H30-9	30	W-5	W	3	5mm/min	400

Plunge tests were executed per the test plan in Table 1 and the schematic shown in Figure 6. A total of five sheets were evaluated, four that had undergone various levels of thermohydrogen processing and one baseline commercially pure variant. A minimum

of six plunges were made in each sheet; thus, allowing both the H-13 and tungsten tool materials to be tested at least three times in each material condition.

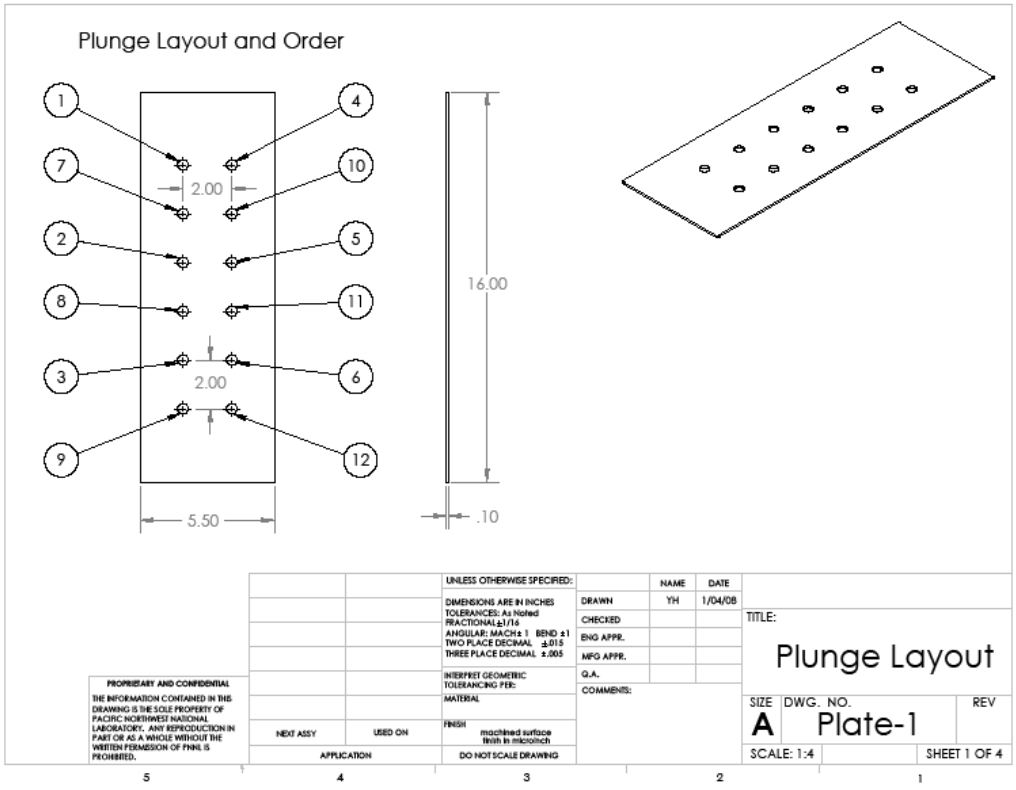

Figure 6. Schematic layout of plunge tests, showing the minimum 50 mm (2 inch) spacing between plunge locations on the titanium sheet.

CHAPTER THREE

ANALYSIS AND DISCUSSION OF RESULTS

Controlled Alloying of Titanium Sheet with Hydrogen

As each of the titanium sheets was wrapped in titanium foil prior to undergoing the hydrogen alloying process, some question as to the uniformity of the hydrogen distribution in the final wrapped sheets existed. Nevertheless, in all cases the hydrogen gas was found to react uniformly with both the outer foil and inner sheet. This was verified by examining both the individual and composite mass increases of the titanium sheet and titanium foil wrappings. The actual measured weights and hydrogen contents of the unwrapped titanium sheets are presented in Table 2, in which the alloyed masses are presented based on an empirical balance from elemental analysis. A complete molar breakdown is presented in detail in Appendix B.

Having wrapped each sheet with foil to getter impurities present in the hydrogen gas supply and furnace atmosphere, the overall foil integrity was crucial to prevent increased surface oxidation during the alloying process. The integrity of the wrapped foil was shown to be adequate in all trials except the 30% atomic case in which the distortion of both the plate and foil during the alloying process led to severe cracking and fracture of the outer foil. This was attributed to the macroscopic distortion related to lattice changes during cooling in which the bcc β phase transforms to the α + β and subsequent α + δ phases as was discussed in previous studies [40-42]. Nevertheless, even with the

failed integrity of the titanium foil in this case, the overall sheet and foil demonstrated uniform absorption of hydrogen as determined from the individual mass increases.

Table 2. Specimen weight targets and actual weights used to determine hydrogen content in thermohydrogen processed commercially pure titanium sheet.

Target (% atomic)	Initial Mass (grams)	Final Mass (grams)	Actual (% atomic)
5	693.43	694.27	5.44
10	694.37	695.95	9.75
20	691.64	695.5	20.96
30	684.1	689.49	27.24

Wrapped specimens were initially taken to 800°C during the alloying process in order accelerate the rate of absorption and diffusion of hydrogen in the titanium. This temperature range was used to better utilize the more favorable kinetics of hydrogen absorption and diffusivity at higher temperatures. While the overall solubility of hydrogen is lower at 800°C than at temperatures below 500°C, the beneficial increases in diffusivity and surface reactivity were found to promote the initial alloying process. Once this reaction was initiated, the temperature was reduced to take advantage of the increased solubility at lower temperatures. At a temperature of 350°C all remaining hydrogen was found to react with the titanium. This reaction was determined to be complete when the pressure increase related to the addition of a fixed mass of hydrogen in the vacuum chamber was eliminated due to the reaction of the gas into the titanium solid.

As one of the most commonly voiced concerns related to temporary alloying of titanium with hydrogen involves the restoration of the original material properties of the titanium metal after removal of the hydrogen, several tests were performed to

demonstrate the post vacuum annealed properties of commercially pure titanium sheet. Stress-strain curves of two distinct sheets used in this project were made using specimens that had undergone a low temperature vacuum anneal having previously been alloyed with hydrogen. This data shown in Figure 7 along with the accompanying picture of the as tested specimens in Figure 8 seem to demonstrate that baseline ductility and strength have been restored. In view of the fact that such results are well documented in the literature for numerous alloys and hydrogen reduction techniques, no additional testing was performed to verify that pre-alloyed properties could be restored.

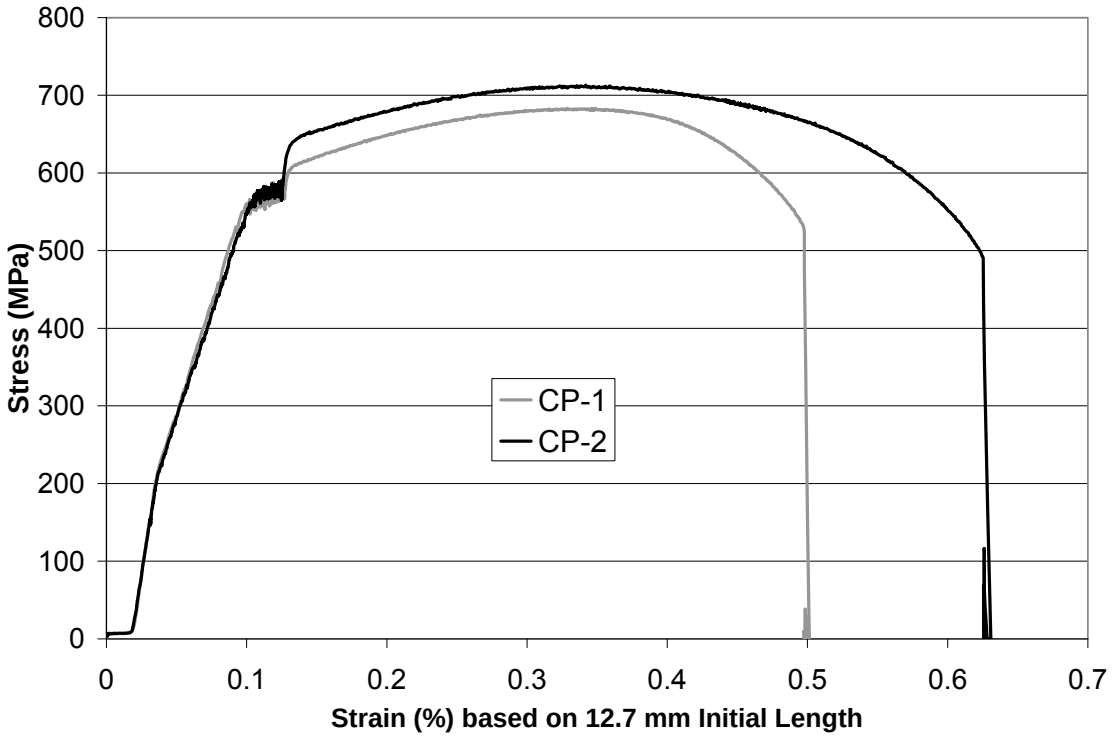

Figure 7. Stress-Strain curve of dehydrided commercially pure titanium sheet. Yield Stress of more than 400 MPa with a 48% area reduction.

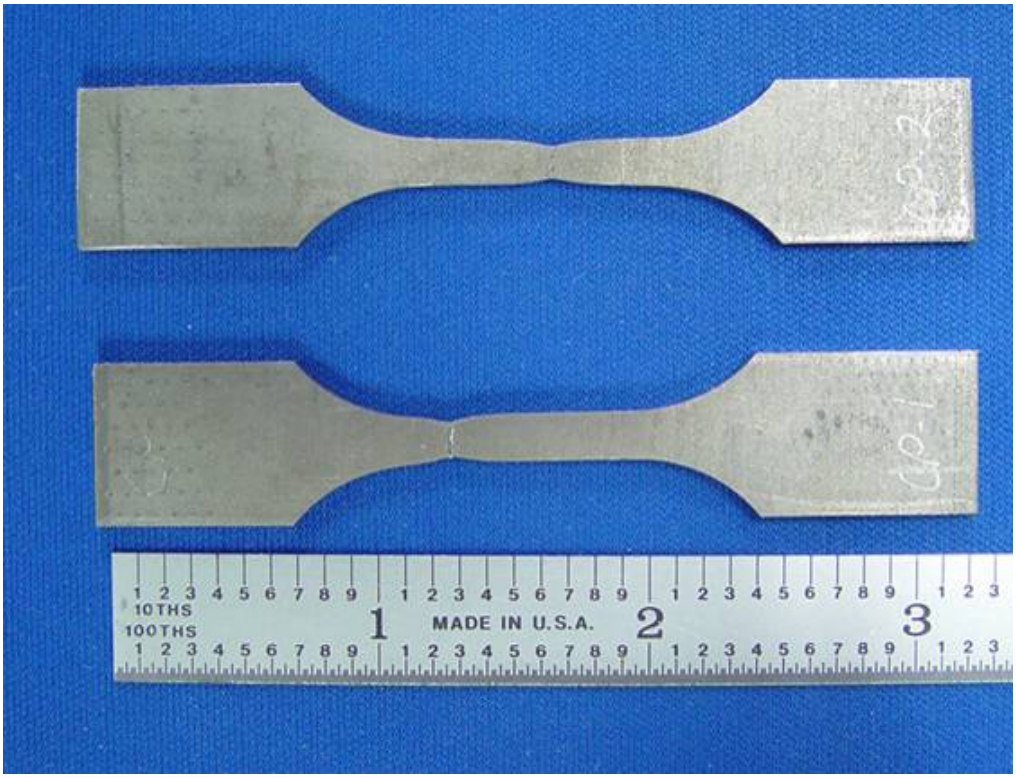

Figure 8. As-tested tensile specimens of dehydrided commercially pure titanium.

Tool Performance

As plunge parameters were held constant for all testing, variability in the resulting data is related to the differing hydrogen content of the sheet as well as the differences in tool materials. A new tool was used with each sheet, and a total of three plunges were made with each tool material in all five titanium sheets. Performance of the tungsten and steel tools deviated greatly based on the overall hydrogen content of the base metal.

Tungsten tools demonstrated the best performance in commercially pure titanium that had been alloyed to a level of 10% atomic hydrogen. With this relatively small addition of hydrogen absorbed into the base material, no measurable deformation of the pin was detected. As previously cited, tungsten based tools used in commercial titanium and its alloys generally lead to deformation of the pin during the plunge phase. Such was

also witnessed herein, as plunging of tungsten tools in commercially pure titanium deformed the pin, effectively "mushrooming" or reducing the overall pin length. After a total of three plunges the pin length had effectively been reduced by approximately 17% from 1.651 to 1.361 mm.

Each of the three tungsten tools used for experiments in the titanium sheet containing 10, 20 and 30 atomic percent hydrogen demonstrated comparable performance, with the hydrogen alloyed titanium building up on the ends of the pins as shown in Figure 9. While this was problematic for repetitive plunging, simple translation was shown to remove such buildup in all cases. While no concentrated effort to develop traverse feed rates was made, some translation with tungsten tools demonstrated that buildup from repetitive plunging was quickly removed at the initiation of lateral movement.

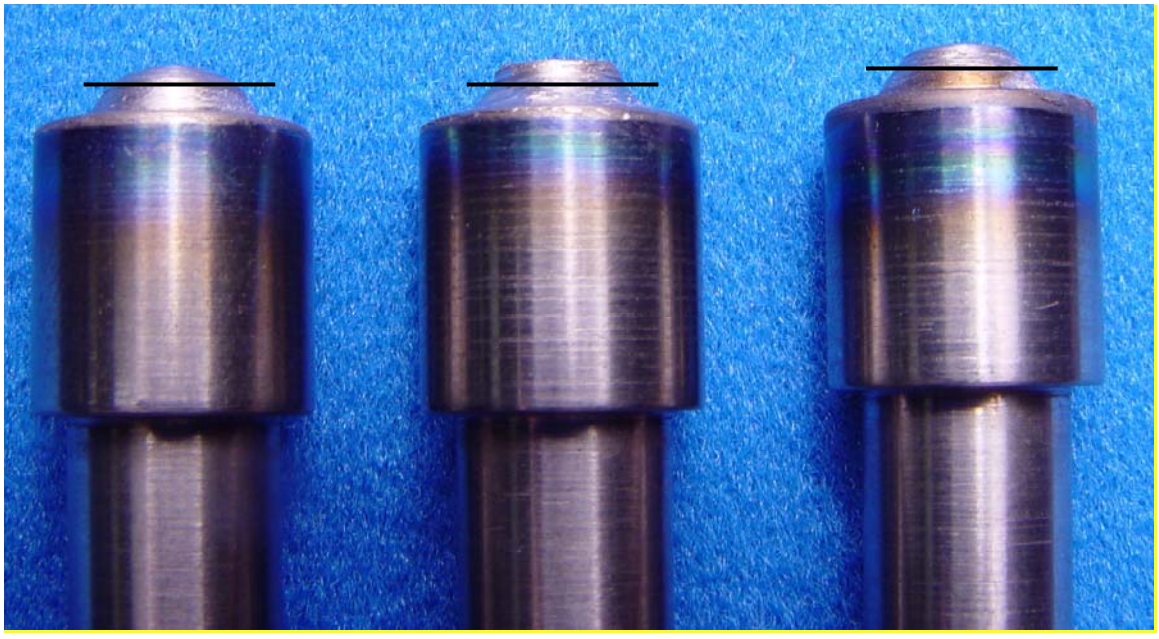

Figure 9. Material buildup on tungsten tools after three FSW plunge tests in CP-Ti alloyed with 10 (left), 20 (middle) and 30 (right) atomic percent hydrogen.

Generally speaking tungsten materials performed better than the steel showing less oxidation, deformation, chemical sensitivity and wear. The H-13 steel tool used with commercially pure titanium was deformed at the shoulder and pin effectively "mushrooming" any surface that came in contact with the titanium sheet. Hydrogen contents of both 20% and 30% atomic, led to significant wear and chemical reactivity between the steel tool and the basemetal. Steel tools demonstrated the best performance in titanium alloyed with hydrogen at a level of 5% and 10% atomic. In both of these conditions, the H-13 tools showed little to no measureable deformation. More significant chemical reactivity was noticed in the 10 % atomic loading condition, as the tool material showed oxidation and material buildup on the surface of the pin and shoulder. The steel tool utilized for testing the titanium alloyed with 5% atomic hydrogen revealed no distinguishable wear after three plunges. While the surface of this tool displayed visible oxidation, it was not damaged by deformation and wear that hampered this tool material in all other test cases.

Friction Stir Welding Plunge Testing

Just as the actual tool performance deviated greatly with variation in hydrogen content and material, the resulting loads were also distinctively unique. Both hydrogen content and tool material greatly influenced the stability and magnitude of the reactive forces and torques. Appendices C and D contain a complete set of graphs plotting the reactive forces and torques for each test case evaluated in this study.

As three individual plunge tests were performed in each titanium sheet, variation from plunge to plunge was quite probable especially due to the extent of wear detected in

the tools used for several of the test conditions. While deviation based on tool deformation and wear from test to test seemed highly plausible, in actuality very little variation was observed. Figure 10 shows z-axis load data for the three plunge set that demonstrated the greatest divergence in all the recorded plunge forces. Such deviation was noticed for this case in which the tool shape was significantly worn and deformed by successive plunging of an H-13 tool in titanium alloyed with 20% atomic hydrogen as shown in Figure 11.

While individually the point by point differences in magnitude are significant as demonstrated by the real-time force plots shown in Figure 10 (a), the overall maximum loads and force trend lines actually show very little variation in peak magnitudes. Figure 10 (b) shows plots of the trend lines for the force data presented in Figure 10 (a). With the initial maximum loads of each trend line showing nearly identical peaks, the test by test deviation may be explained by the deformation of the tool that increased with each subsequent test. For the set of data shown in Figure 10, test 13 was run first followed in numerical order by test 14 and 15. The magnitude of the load from test to test during the 7 to 15 second time range increased with each test, which may also be related to the additional buildup of material on the tool pin and shoulder as well as the overall deformation of the tool. Such assumptions also help to explain the divergence in load magnitudes during the last five seconds, which seem to be adversely affected by the increasing length of the pin resulting from material buildup.

Comparative measurements of all other load data sets demonstrated less variation than that shown in Figure 10, and as such all additional data is presented individually without further comment on test specific divergence.

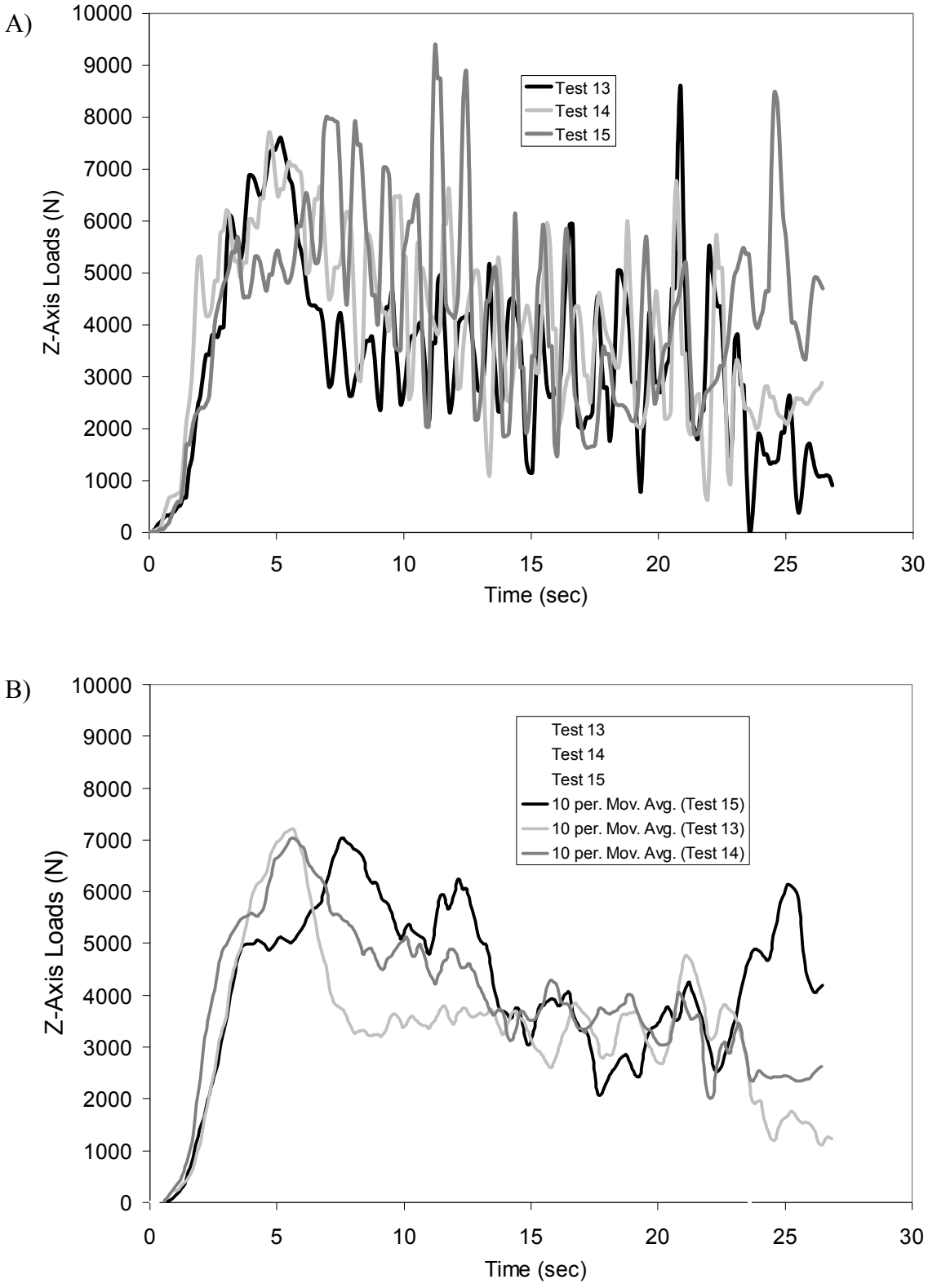

Figure 10. Tool reaction loads showing the increased data scatter for hydrogen contents above 10 atomic percent.

Figure 11. H-13 friction stir welding tool after three plunges in titanium sheet alloyed with 20% atomic hydrogen.

Average peak magnitudes for tool reaction forces and torques along with the standard deviation of the set are presented in Table 3. An additional column in Table 3 presents comparative data showing the average percent reduction in the peak magnitude of the plunge force in thermal hydrogen processed titanium from the commercially pure equivalent. As the intent of temporarily adding hydrogen to the titanium sheet was to facilitate the friction stir process, reducing the overall plunge loads to avoid tool deformation and wear was desirable.

Table 3. Tabulated values of average peak loads and average peak torques recorded during FSW plunge tests in thermohydrogen processed commercially pure titanium sheets.

Plate ID	Max Torque (N-m)	Standard Deviation (N-m)	Max Z-Force (kN)	Standard Deviation (kN)	Force Reduction (%)
Tungsten Tooling					
Cp-Ti	23.3	0.8	16.2	0.11	NA
Plate #1 (10% H)	26.4	2.74	11.86	0.46	26.8
Plate #2 (20% H)	20.7	0.32	11.34	1.2	30
Plate #3 (5% H)	24.3	0.68	12.35	0.89	23.8
Plate #4 (30% H)	24.1	3.06	11.32	0.57	30.1
H-13 Tooling					
Cp-Ti	19.08	0.35	11.04	0.4	NA
Plate #1 (10% H)	16.97	5.12	8.53	0.8	22.8
Plate #2 (20% H)	17.64	4.62	8.55	0.83	22.6
Plate #3 (5% H)	20.03	1.7	9.42	0.34	14.7
Plate #4 (30% H)	17.8	1.8	7.83	0.89	29.1

Effect of Hydrogen on Flow Stress in Commercially Pure Titanium

As there are numerous methodologies that may be employed to reduce the applicable flow stresses relevant to a discussion on friction stir welding titanium, a more detailed look at the influence of hydrogen and temperature on the phase kinetics and flow stresses applicable to the friction stir regime seems appropriate.

The hcp α-phase transition to bcc β phase at 882°C in commercially pure titanium produces a sizable reduction in both the yield and flow stresses of commercially pure titanium alloys. Senkov and others [12, 21] demonstrated the yield stress of an α-phase commercially pure titanium at 800°C exceeded 40 MPa, yet an increase over the β transition temperature to 900°C reduced the yield stress to less than 15 MPa. A similar

reduction in yield stress was demonstrated without increasing the temperature, but instead increasing the hydrogen content adequately to drop the β transition temperature below the 800°C threshold. For the case in point a hydrogen content of 9% atomic resulted in a reduction of the yield stress at 800°C to a level comparable with commercially pure titanium at 900°C [12, 21]. The influence of increasing temperature and hydrogen content had an even more dramatic effect on the reduction of flow stresses in titanium. A 9% atomic increase in hydrogen reduced the flow stress at 800°C from 110 MPa to below 50 MPa, while an increase in temperature from 800°C to 900°C exhibited a similar effect [12].

Significant reductions in both yield stress and flow stress can be realized with increasing hydrogen content of both the α and α + β phases. Conversely, an increase in the hydrogen content of β phase titanium produces a deleterious effect on overall stress reduction [12, 18-21]. Senkov [12] showed that any increase in hydrogen content of β phase titanium yielded an increase in the yield stress and flow stress at temperatures ranging from 500°C to 920°C. Furthermore, he demonstrated that the effective escalation in flow stress with increasing hydrogen was exacerbated at increasing strain rates, having evaluated strain rates from 0.001/second to 1.0/second. This rise in the flow stress related to increasing hydrogen concentration was tempered for hydrogen concentrations below 10% atomic, but exponentially increased as hydrogen concentrations were increased to 30% atomic and beyond [12].

Previous experiments in FSW titanium alloys show that peak weld temperatures vary between 700°C and 1000°C, which indicates that the greatest reductions in flow stress may be achieved at hydrogen contents ranging between 9% atomic and 15% atomic

based on the results previously discussed from others [12, 18-21]. Senkov and others also demonstrated that at 700°C and 15% atomic hydrogen, commercially pure titanium is β-phase stabilized with a flow stress minimum of below 70 MPa for strain rates of 1.0 s^{-1}. They also showed that increasing the temperature to 800°C or 900°C only reduces the effective flow stress by 20 MPa per 100°C interval, yet a reduction to 600°C increases the same by more than 50 MPa and transitions back to the α + β phase. Thus, increasing the hydrogen content of the basemetal sufficiently to stabilize the β-phase for the applicable thermal regime would lead to increased stability while reducing the z-axis reaction loads.

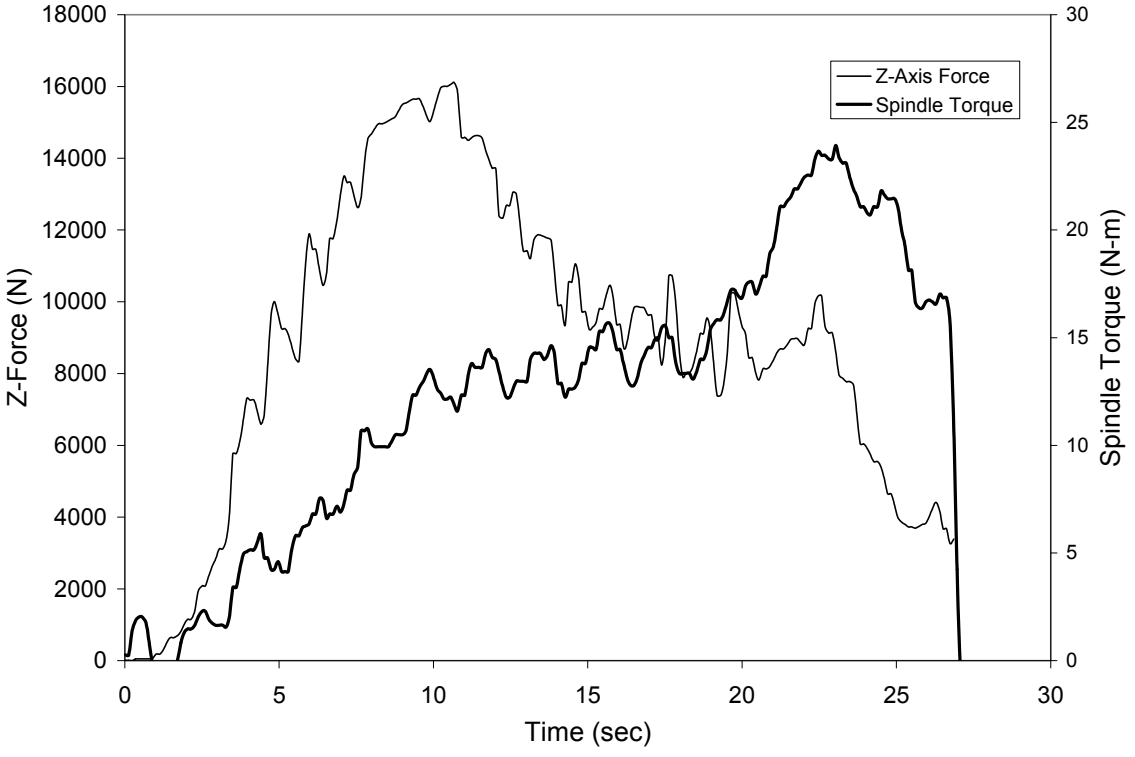

Figure 12. Load and torque magnitudes for a FSW plunge test using a tungsten tool in commercially pure titanium sheet.

Plots of tool loads and torques are presented in Figures 12 thru 15, demonstrating the effect of thermohydrogen processing on tool loads during the plunge phase of friction stir welding. While peak values were previously reported in Table 3, the transient nature of the plunge phase influences the overall process loads and torques throughout the 25 second duration. Tool reaction loads are generally highest during the initial portion of the plunge, and this is also the segment that has the lowest temperatures. As the tool continues to plunge into the basemetal, friction and pressure begin to heat the sheet, effectively plasticizing a portion of the material around the tool. The increased temperature of this stirred region directly benefits from the resulting stress reductions association with the addition of hydrogen.

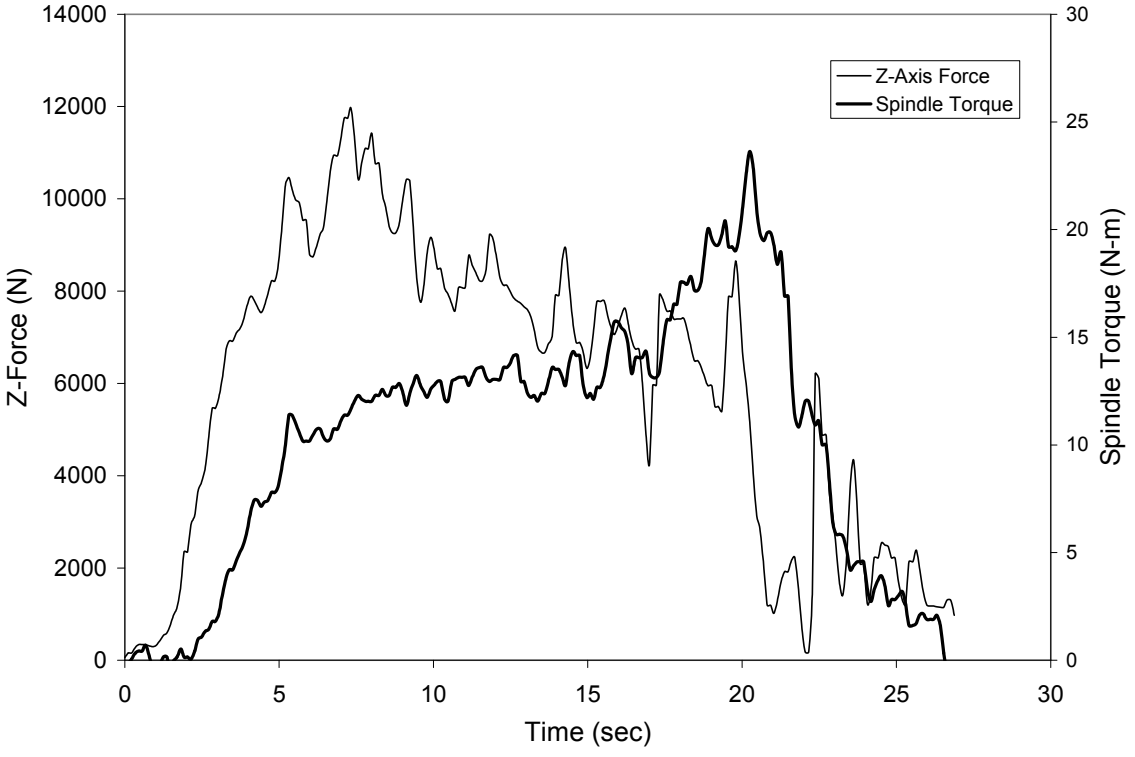

Figure 13. Load and torque magnitudes for a FSW plunge test using a tungsten tool in titanium sheet alloyed to 10% atomic hydrogen.

Increased hydrogen content yields reductions in the average tool reaction forces at the end of the plunge; however, the overall uniformity of the load magnitude or stability of the reaction to the tool plunge seems to diminish for hydrogen contents above 10% atomic. This may be related to the overall increased embrittlement of the titanium for increasing contents of hydrogen. Such changes in the ductility of the material may be leading to more incremental brittle failure mechanisms that tend to generate less uniform load profiles.

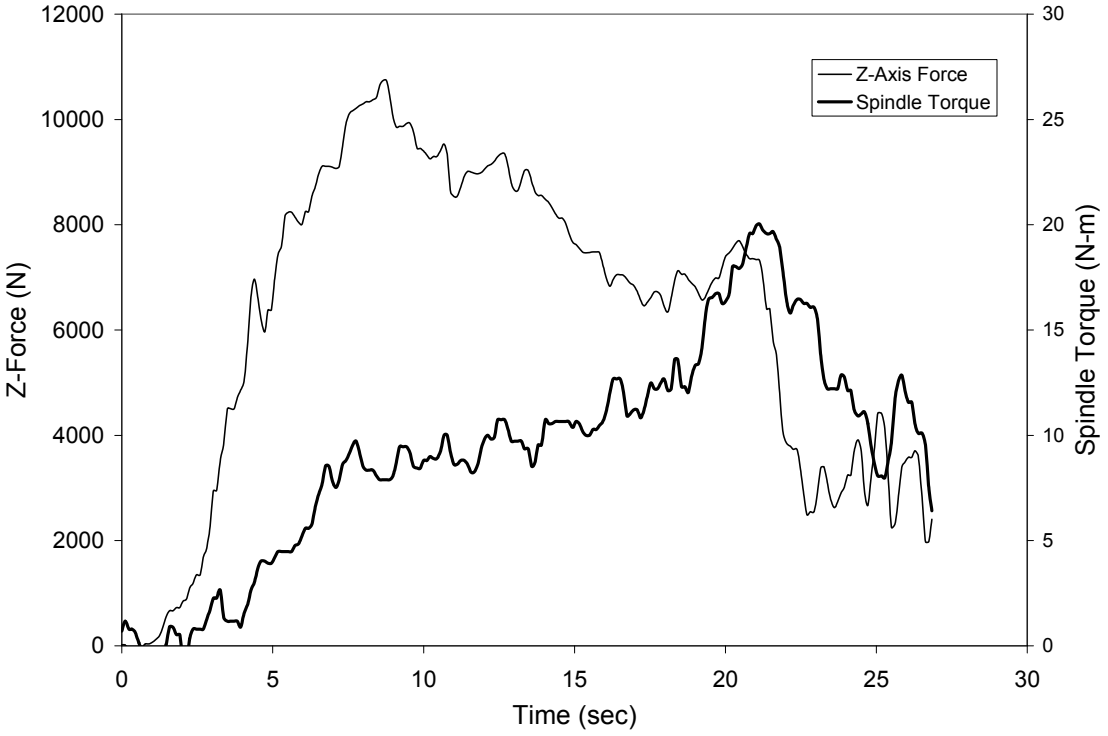

Figure 14. Load and torque magnitudes for a FSW plunge test using an H-13 tool in commercially pure titanium sheet.

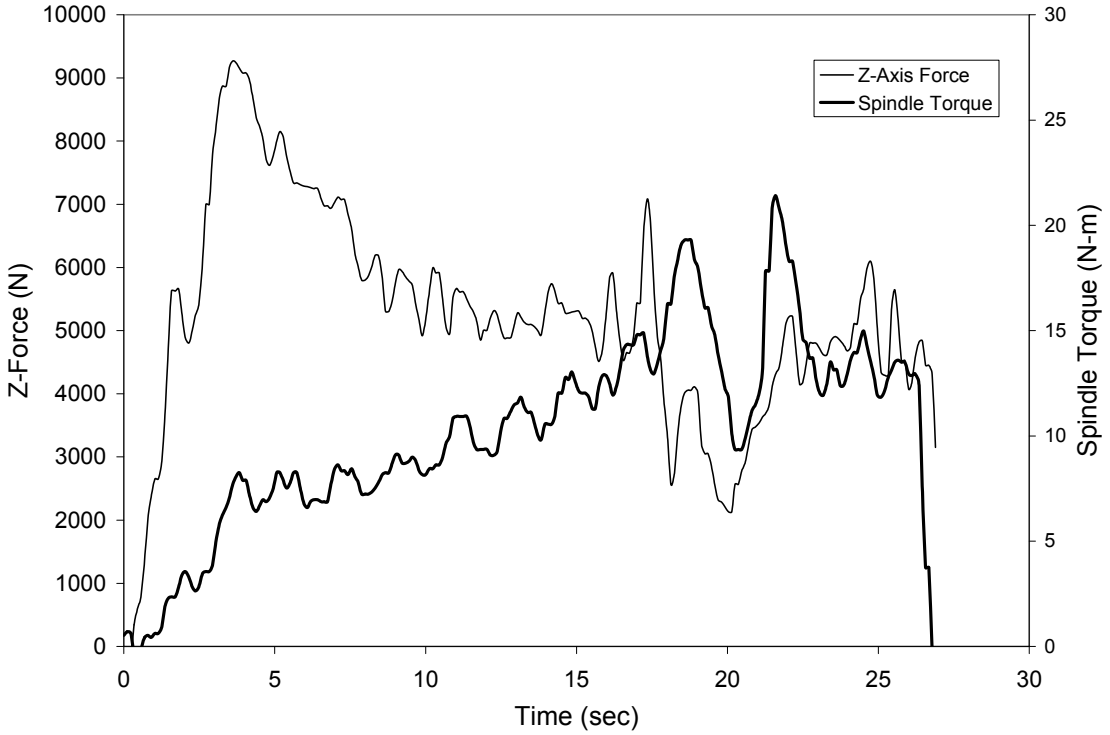

Figure 15. Load and torque magnitudes for a FSW plunge test using an H-13 tool in titanium sheet alloyed to 5% atomic hydrogen.

CHAPTER FOUR

CONCLUSIONS AND FUTURE RECOMMENDATIONS

While historically hydrogen has been considered an impurity in titanium, when used as a temporary alloying agent it promotes beneficial changes to material properties that increase the hot-workability of the metal. This thermohydrogen processing technique was used to temporarily alloy hydrogen with commercially pure titanium sheet as a means of facilitating the FSW process. Specific alloying parameters were developed to increase the overall hydrogen content of the titanium sheet ranging from commercially pure to 30 atomic percent. Two materials, H-13 tool steel and pure tungsten, were used to fabricate FSW tools that were plunged into each of the thermohydrogen processed titanium sheets. The effects of hydrogen addition on the process loads throughout the plunge sequence were observed, and tool wear was characterized to determine the effect of the tool material reactions with the weld metal. The following conclusions resulted from the data and analysis obtained throughout this study:

1. Thermohydrogen processing of commercially pure titanium facilitates a reduction in the initial tool reaction forces during the plunge phase of the FSW process.
2. The effect of hydrogen concentration was unique to each tool material. The most stable response with H-13 tooling was at 5% atomic hydrogen, while a 10% atomic hydrogen concentration proved more effective with tungsten tools.
3. Thermohydrogen processing conditions that produced the least wear for a given tool also showed the greatest process stability as demonstrated by less fluctuation in the

4. Hydrogen loading above 10 percent atomic led to increased variability, often to a point of instability, in the tool reaction forces during the later portion of the plunge regardless of tool material used in this study.

Future Recommendations

Despite the fact that the data presented herein demonstrated that thermohydrogen processing can be utilized to facilitate the friction stir welding process in titanium, there remains many questions about the overall benefit gained and final properties attained. While it was beyond the scope of the current research to provide a detailed post weld study of the material properties of thermohydrogen processed friction stir welded titanium, the detail provided herein should serve as a stepping stone in selecting the applicable hydrogen loading for a material/tool combination necessary to produce linear friction stir welds. Additionally, this work could be furthered by elaborating on the actual thermal conditions specific to FSW in each hydrogen alloyed condition.

BIBLIOGRAPHY

1. Thomas, W. M. et. al., 1991, "Friction Stir Butt Welding, International Patent Application PCT/GB92/02203, GB Patent Application No. 9125978.8 and U.S. Patent No. 5,460,317.

2. Goetz, R. L., and Jata, K. V., 2001, "Modeling Friction Stir Welding of Titanium and Aluminum Alloys," Proc. Friction Stir Welding and Processing, K. V. Jata et al., eds., TMS annual meeting, pp. 35-42.

3. Smith, C.B., Hinrichs, J.F., and Ruehl, P.C., "Friction Stir and Friction Stir Spot Welding – Lean, Mean and Green," Internal Publication to Friction Stir Link, Inc. W227 N546 Westmound Dr., Waukesha, WI 53186.

4. Mishra, R.S., and Mahoney, M.W., 2007, "Friction Stir Welding and Processing," ASM International, Materials Park, OH, Chapters 2, 4, and 6-9.

5. Christodoulou, L., 2008, "DARPA Initiative in Titanium," Defense Sciences Office thrust area, http://darpa.mil/dso/thrusts/materials/novelmet/titanium/index.htm.

6. Jones, R. E., and Loftus, Z. S., 2006, "Friction Stir Welding of 5mm Titanium 6Al-4V," Proc. MS&T Joining of Advanced and Specialty Materials, T.J. Lienert et al. organizers, pp. 119-129.

7. Rubisoff, H. Querin, J. and Schneider, M.J., 2008, "Microstructural Evolution in Friction Stir Welding of Ti-6Al-4V," MS&T, Pittsburgh PA.

8. Lee, W., Lee, C., Chang, W., Yeon, Y., and Jung, S., 2005, "Microstructural investigation of friction stir welded pure titanium," Materials Letters, **59**, pp. 3315-3318.

9. Ramirez, A. J., and Juhas, M. C., 2003, "Microstructural Evolution in Ti-6Al-4V Friction Stir Welds," Materials Science Forums, **426-432**, pp. 2999-3004.

10. Reynolds, A. P., Hood, E., and Tang, W., 2004, "Texture in friction stir welds of Timetal 21S," Scripa Materialia, **52**, pp. 491-494.

11. Trapp, T., Helder, E., and Subramanian, P. R., 2003, "FSW of Titanium Alloys for Aircraft Engine Components," Proc. Friction Stir Welding and Processing II, K.V. Jata et al., eds., TMS annual meeting, pp. 173-178.

12. Senkov, O. N. and Jonas, J. J., 1996, "Effect of Phase Composition and Hydrogen Level on the Deformation Behavior of Titanium-Hydrogen Alloys," Metallurgical and Materials Transactions A, 27A, pp. 1869-1876.

13. Senkov, O. N. and Jonas, J. J., 1996, "Dynamic Strain Aging and Hydrogen-Induced Softening in Alpha Titanium," Metallurgical and Materials Transactions A, 27A, pp. 1877-1887.

14. Zhang, S., 2001, "Hydrogenation Behavior, Microstructure and Hydrogen Treatment for Titanium Alloys," *Progress in Hydrogen Treatment of Metals*, V. A. Goltsov eds.

15. Tal-Gutelmacher, E., and Eliezer, D., 2005, "High Fugacity Hydrogen Effects at Room Temperature in Titanium Based Alloys," J. of Alloys and Compounds, **404-406**, pp. 613-616.

16. Setoyam, D., Matsunaga, J., Muta, H., Uno, M., and Yamanaka, S., 2004, "Characteristics of Titanium-Hydrogen Solid Solution," J. of Alloys and Compounds, **385**, pp. 156-159.

17. Schur, D. V., Zaginaichenko, S. Y., Adejev, V. M., Voitovich, V. B., Lyashenko, A. A., and Trefilov, V. I., 1996, "Phase Transformations in Titanium Hydrides," Int. J. Hydrogen Energy, **21** (11/12), pp. 1121-1124.

18. Christ, H. J., Senemmar, A., Decker, M., and PRÜBNER, K., 2003, "Effect of Hydrogen on Mechanical Properties of β –Titanium Alloys," Sādhanā, **28** (3-4), pp. 453-465.

19. Yoshimura, H., 1997, "Mezzoscopic Grain Refinement and Improved Mechanical Properties of Titanium Materials by Hydrogen Treatments," Int. J. Hydrogen Energy, **22** (2/3), pp. 145-150.

20. Senkov, O. N., and Froes, F. H., 1999, "Thermohydrogen Processing of Titanium Alloys," Int. J. of Hydrogen Energy, **24**, 565-576.

21. Senkov, O. N., and Froes, F. H., 2001, "Hydrogen as a Temporary Alloying Element in Titanium Alloys," *Progress in Hydrogen Treatment of Metals*, V. A. Goltsov eds.

22. Zwigl, P., and Dunand, D. C., 2001, "Internal-Stress Plasticity in Titanium by Cyclic Alloying/Dealloying with Hydrogen," J. of Materials Processing Tech., **117**, pp. 409-417.

23. Murzinova, M. A., Salishchev, G. A., and Afonichev, D. D., 2002, "Formation of Nanocrystalline Structure in Two-Phase Titanium Alloy by Combination of Thermohydrogen Processing with Hot Working," International J. of Hydrogen Energy, **27**, pp775-782.

24. Ilyin, A. A., Kolachev, B. A., and Nosov, V. K., 2001, "The Achievement and Prospects of Hydrogen Technology of Titanium Alloys Production and Treatment," *Progress in Hydrogen Treatment of Metals*, V. A. Goltsov eds.

25. Ilyin, A. A., Skvortsova, S. V., Mamonov, A. M., Permyakova, G. V., and Kurnikov, D. A., 2002, "Effect of Thermohydrogen Treatment on the Structure and Properties of Titanium Alloy Castings," Metal Science and Heat Treatment, **44** (5-6), pp. 185-189.

26. Eliaz, N., Eliezer, D., and Olson, D. L., 2000, "Hydrogen-Assisted Processing of Materials," Materials Science and Engineering, **A289**, pp. 41-53.

27. Eliezer, D., Eliaz, N., Senkov, O. N., and Froes, F. H. 2000, "Positive Effects of Hydrogen in Metals," Materials Science and Engineering, **A280**, pp 220-224.

28. Aksyonov, Y. A., Anisimova, L. I., and Kolmogorov, V. L., 1994, "Reversible Addition of Hydrogen to Titanium Alloys," J. Mat. Processing Tech., **40**, pp. 477-489.

29. Bhosle, V., Baburaj, E. G., Miranova, M., and Salama, K., 2003, "Dehyrogenation of TiH_2," Materials and Engineering, **A356**, pp. 190-199.

30. Evard, E. A., Gavis, I. E., and Voyt, A. P., 2005, "Study of the Kinetics of Hydrogen Sorption and Desorption from Titanium," J. of Alloys and Compounds, **404-406**, pp. 335-338.

31. Hirooka, Y., Miyake, M., and Sano, T., 1981, "A Study of Hydrogen Absorption and Desorption by Titanium," J. of Nuclear Materials, **96**, pp. 227-232.

32. Kolachev, B. A., 1993, "Reversible Hydrogen Alloying of Titanium Alloys," Moscow Institute of Aircraft Technology (Stupano Branch), (10), pp. 28-32.

33. Watanabe, T., Takayama, H., and Yanagisawa, A., 2006, "Joining of Aluminum Alloy to Steel by Friction Stir Welding," J. of Mats. Proc. Tech., 178, pp. 342-349.

34. Olayo, M. G., Cruz, G. J., Martinez, T., Melendez, L., Valencia, R., Chavez, E., Flores, A., and Lopez, R., 1998, "Sorption of Hydrogen in Titanium Plates at Low Pressure," Int. J. Hydrogen Energy, **23** (1), pp. 15-18.

35. Williams, D. N., Koehl, B. G., and Bartlett, E. S., 1969, "The Reaction of Titanium with Hydrogen Gas at Ambient Temperatures," J. of the Less-Common Metals, **19**, pp.385-398.

36. Wipf, H., Kappesser, B., and Werner, R., 2000, "Hydrogen Diffusion in Titanium and Zirconium Hydrides," J. of Alloys and Compounds, **310**, pp. 190-195.

37. Korn, C., and Zamir, D., 1972, "On the Model for the Diffusion of Hydrogen in Titanium Hydride," J. Phys. Chem. Solids, **34**, pp. 725-734.

38. Chornet, E., and Coughlin, R. W., 1974, "Kinetic Aspects of the Interaction of Hydrogen with Titanium," Journal of Colloid and Interface Science, **47**(2), pp. 406-415.

39. Millenback, P., and Givon, M., 1983, "Permeation of Hydrogen Through Titanium and Titanium Hydride," J. of the Less-Common Metals, **92**, pp. 339-342.

40. Trefilov, V. I., Timofeeva, I. I., Klochkov, L. I., Morozov, I. A., and Morozova, R. A., 1996, "Effects of Temperature Change and Hydrogen Content on Titanium Hydride Crystal Lattice Volume," Int. J. Hydrogen Energy, **21** (11/12), pp. 1101-1103.

41. Senkov, O. N., Chakoumakos, B. C., Jonas, J. J., and Froes, F. H., 2001, "Effect of Temperature and Hydrogen Concentration on the Lattice Parameter of Beta Titanium," Materials Research Bulletin, **36**, pp. 1431-1440.

42. Chen, C. Q., Li, S. X., Zheng, H., Wang, L. B., and Lu, K., 2004, "An Investigation on Structure, Deformation and Fracture of Hydrides in Titanium with a Large Range of Hydrogen Contents," Acta Materialia, **52**, pp. 3697-3706.

APPENDIX

Appendix A: FSW Tool Drawing

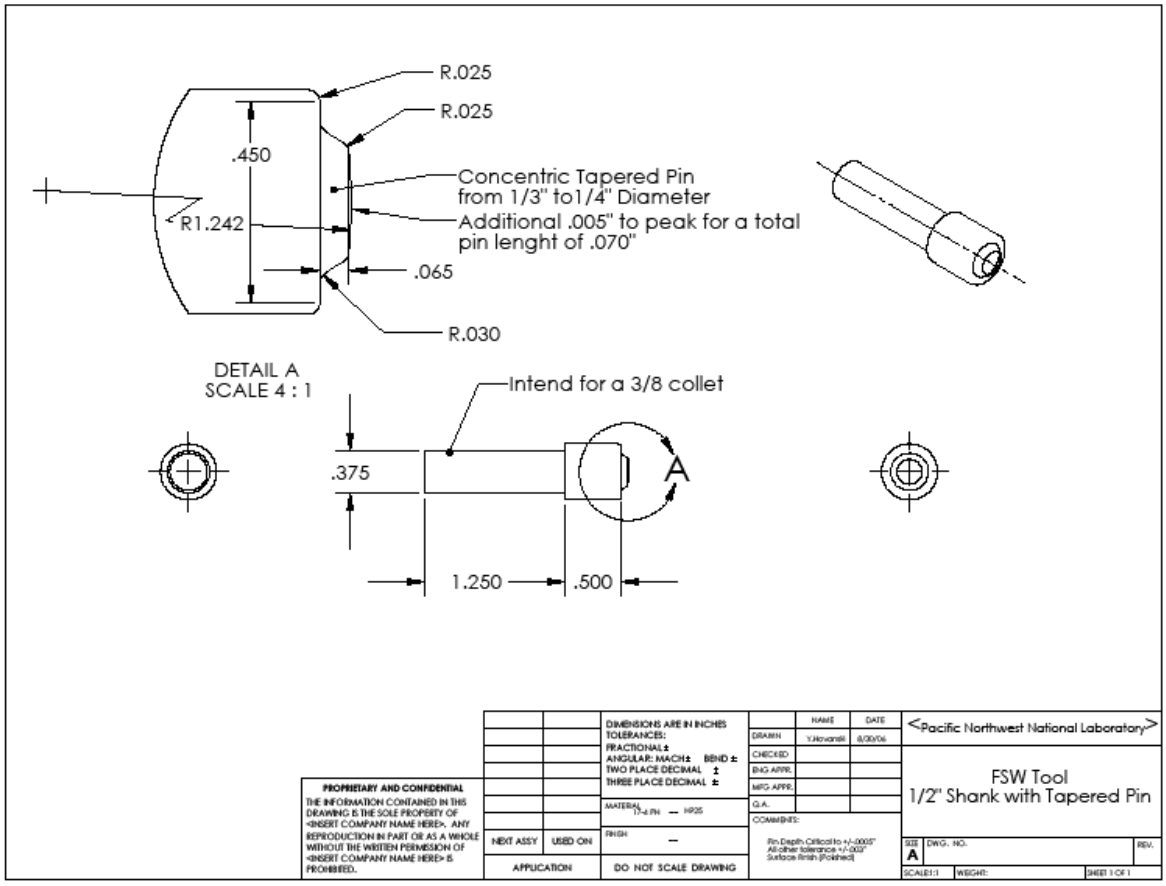

Appendix B: Molar Breakdown of Hydrogen Content

CP-Ti Sheet #1 wrapped in Ti foil (694.37g)

Mass and Atomic Percentages for Titanium-Hydrogen Mixtures

Measured Initial Weight (g)				Desired H		Total	Hydrogen	Hydrogen	Required Hydrogen
Titanium	Aluminum	Vanadium		(at %)		(moles)	(moles)	(mass %)	(g)
694.37	0	0		10		16.11366	1.611366379	0.23%	1.624096173

Elements	Atomic Mass
Ti	47.88
Al	26.982
V	50.942
H	1.0079

Verification Calculator for plate				
Initial Mass in Grams				
Titanium	Aluminum	Vanadium	Hydrogen	Total mass
694.37	0	0	1.58	695.95
Individual Molar Breakdown (moles)				
Titanium	Aluminum	Vanadium	Hydrogen	Total Moles
14.5023	0	0	1.567616	16.06991325
Individual Atomic Percentages (at. %)				
Titanium	Aluminum	Vanadium	Hydrogen	Total Atomic %
90.25%	0.00%	0.00%	9.75%	100.00%

CP-Ti Sheet #2 wrapped in Ti foil (691.64g)

Mass and Atomic Percentages for Titanium-Hydrogen Mixtures

Measured Initial Weight (g)				Desired H		Total	Hydrogen	Hydrogen	Required Hydrogen
Titanium	Aluminum	Vanadium		(at %)		(moles)	(moles of H)	(mass %)	(g)
691.64	0	0		20		18.0566	3.611319967	0.52%	3.639849394

Elements	Atomic Mass
Ti	47.88
Al	26.982
V	50.942
H	1.0079

Verification Calculator for plate				
Initial Mass in Grams				
Titanium	Aluminum	Vanadium	Hydrogen	Total mass
691.64	0	0	3.86	695.5
Individual Molar Breakdown (moles)				
Titanium	Aluminum	Vanadium	Hydrogen	Total Moles
14.44528	0	0	3.829745	18.27502488
Individual Atomic Percentages (at. %)				
Titanium	Aluminum	Vanadium	Hydrogen	Total Atomic %
79.04%	0.00%	0.00%	20.96%	100.00%

CP-Ti Sheet #3 wrapped in Ti foil (693.43g)

Mass and Atomic Percentages for Titanium-Hydrogen Mixtures

Measured Initial Weight (g)				Desired H		Total	Hydrogen	Hydrogen	Required Hydrogen
Titanium	Aluminum	Vanadium		(at %)		(moles)	(moles of H2)	(mass %)	(g)
693.43	0	0		5		15.24491	0.762245526	0.11%	0.768267266

Elements	Atomic Mass
Ti	47.88
Al	26.982
V	50.942
H	1.0079

Verification Calculator for plate				
Initial Mass in Grams				
Titanium	Aluminum	Vanadium	Hydrogen	Total mass
693.43	0	0	0.84	694.27
Individual Molar Breakdown (moles)				
Titanium	Aluminum	Vanadium	Hydrogen	Total Moles
14.48266	0	0	0.833416	15.31608101
Individual Atomic Percentages (at. %)				
Titanium	Aluminum	Vanadium	Hydrogen	Total Atomic %
94.56%	0.00%	0.00%	5.44%	100.00%

CP-Ti Sheet #4 wrapped in Ti foil (684.10g)

Mass and Atomic Percentages for Titanium-Hydrogen Mixtures

Measured Initial Weight (g)				Desired H		Total	Hydrogen	Hydrogen	Required Hydrogen
Titanium	Aluminum	Vanadium		(at %)		(moles)	(moles of H2)	(mass %)	(g)
684.1	0	0		30		20.41115	6.123344074	0.89%	6.171718493

Elements	Atomic Mass
Ti	47.88
Al	26.982
V	50.942
H	1.0079

Verification Calculator for plate				
Initial Mass in Grams				
Titanium	Aluminum	Vanadium	Hydrogen	Total mass
684.1	0	0	5.39	689.49
Individual Molar Breakdown (moles)				
Titanium	Aluminum	Vanadium	Hydrogen	Total Moles
14.2878	0	0	5.347753	19.63555559
Individual Atomic Percentages (at. %)				
Titanium	Aluminum	Vanadium	Hydrogen	Total Atomic %
72.76%	0.00%	0.00%	27.24%	100.00%

Appendix C: Reaction Forces and Torques Using an H-13 Tool

Commercially Pure Titanium

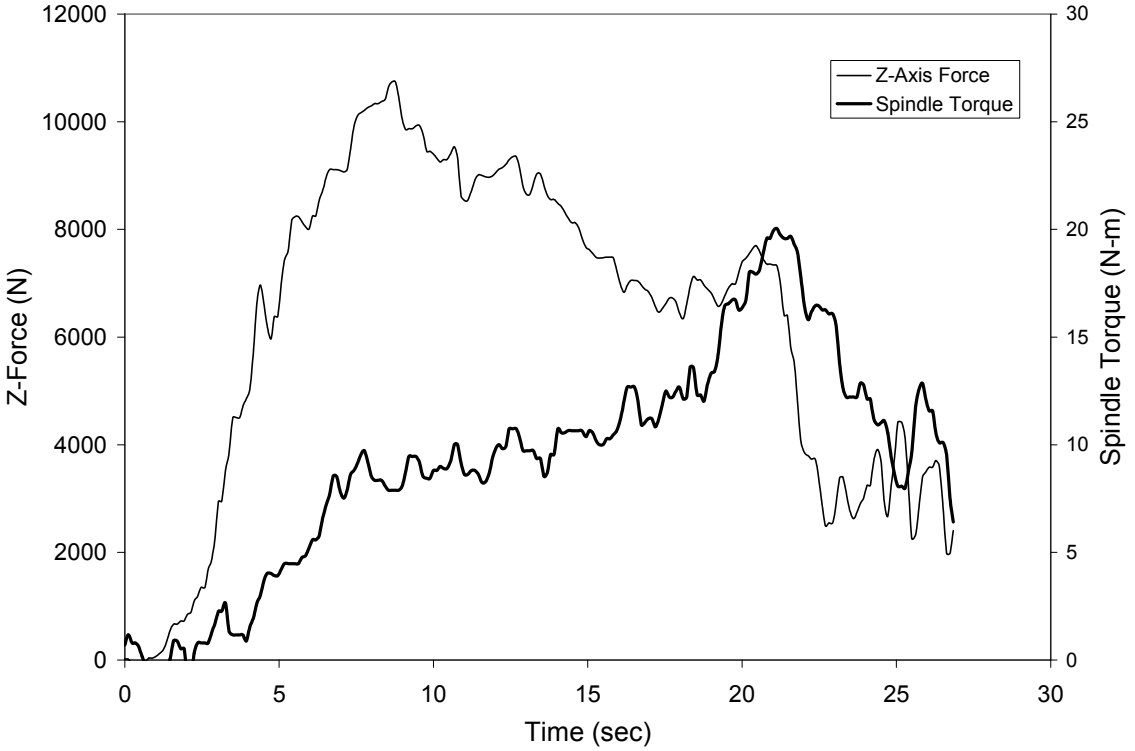

5% Atomic Hydrogen Alloyed CP-Ti

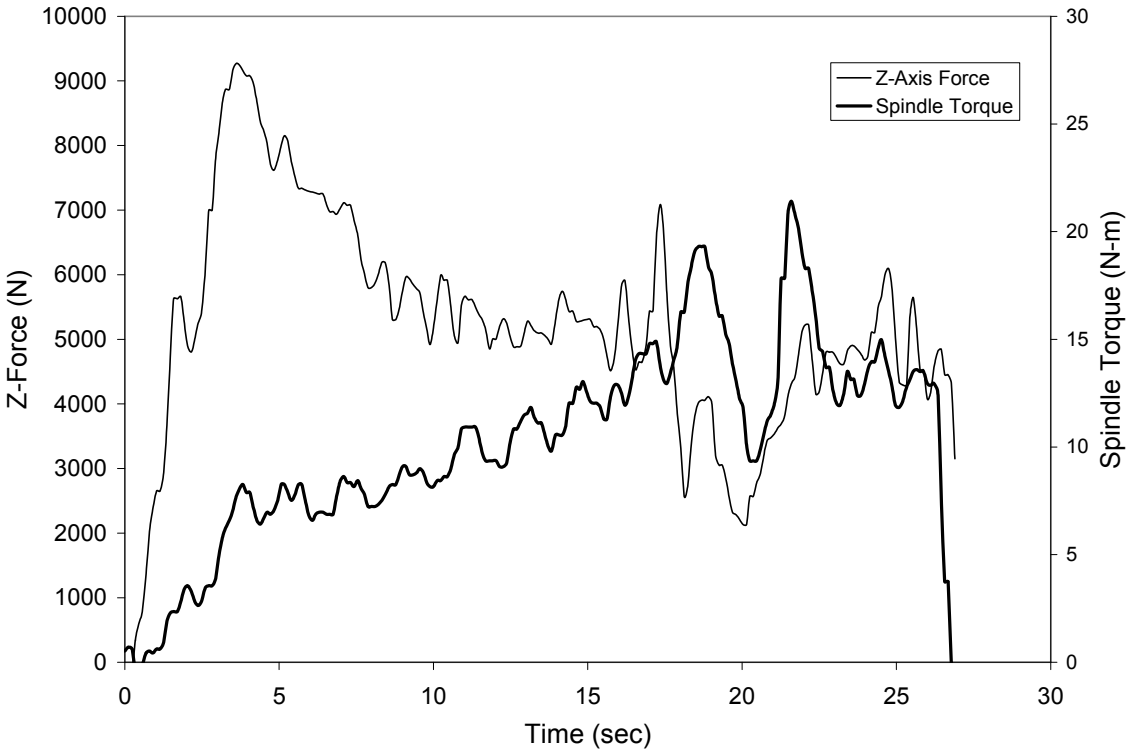

10% Atomic Hydrogen Alloyed CP-Ti

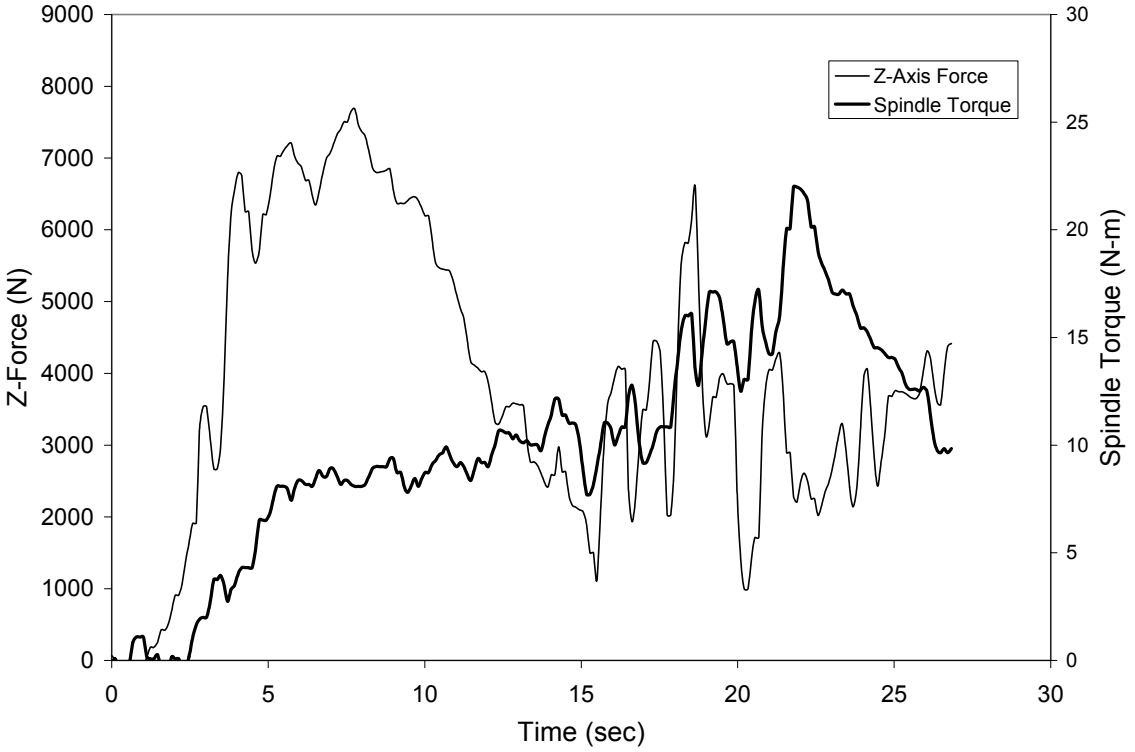

20% Atomic Hydrogen Alloyed CP-Ti

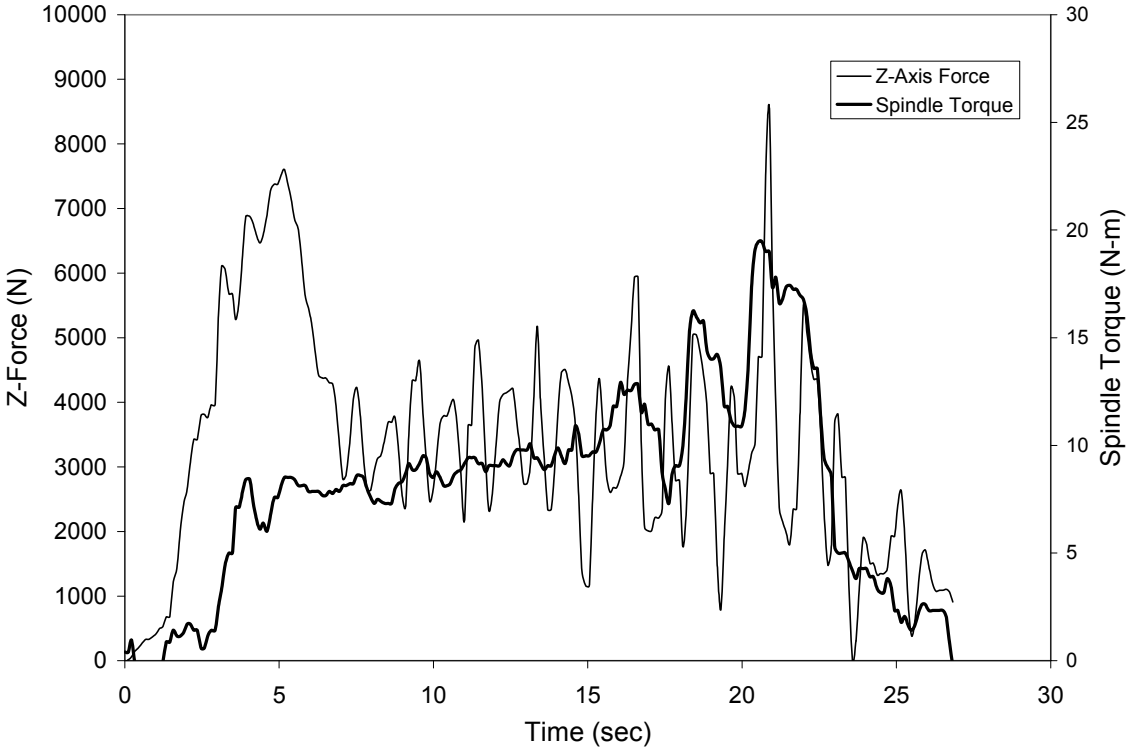

30% Atomic Hydrogen Alloyed CP-Ti

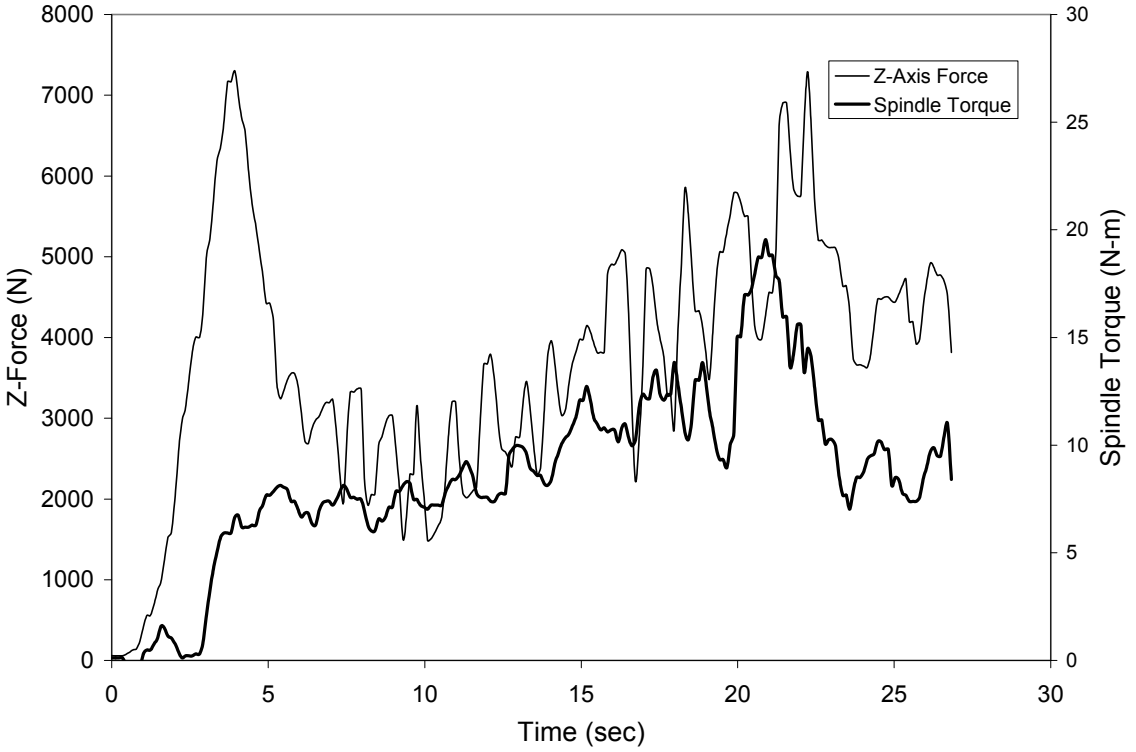

Appendix D: Reaction Forces and Torques Using a Tungsten Tool

Commercially Pure Titanium

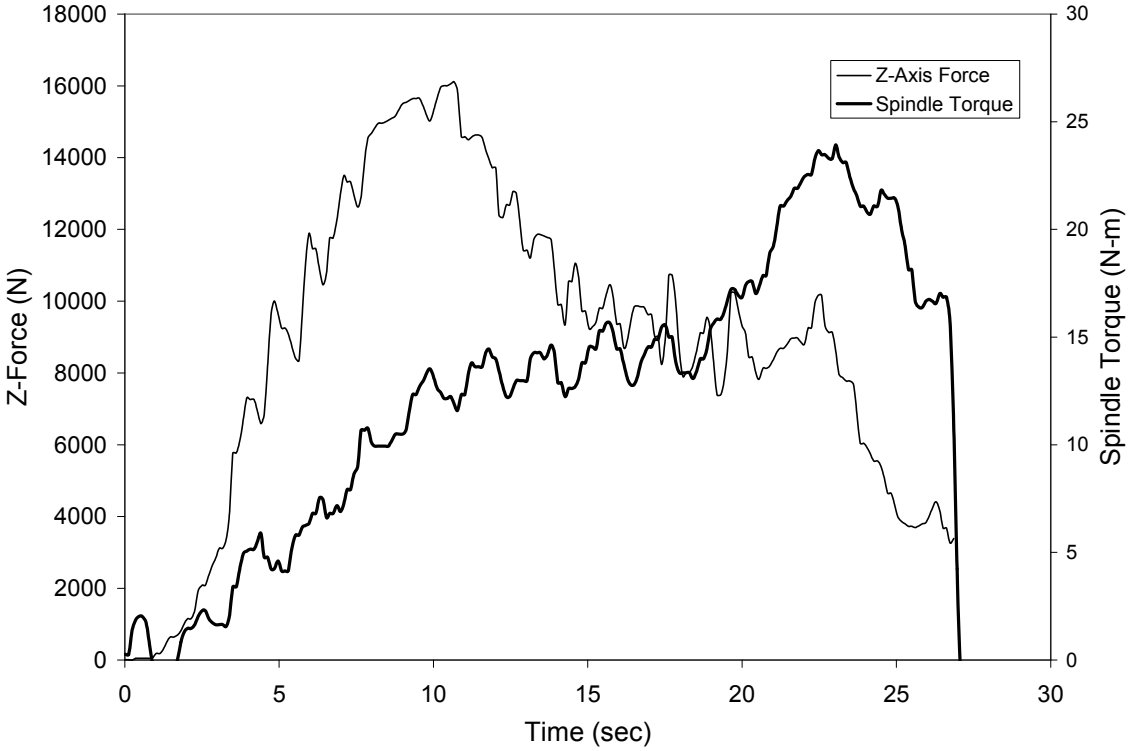

5% Atomic Hydrogen Alloyed CP-Ti

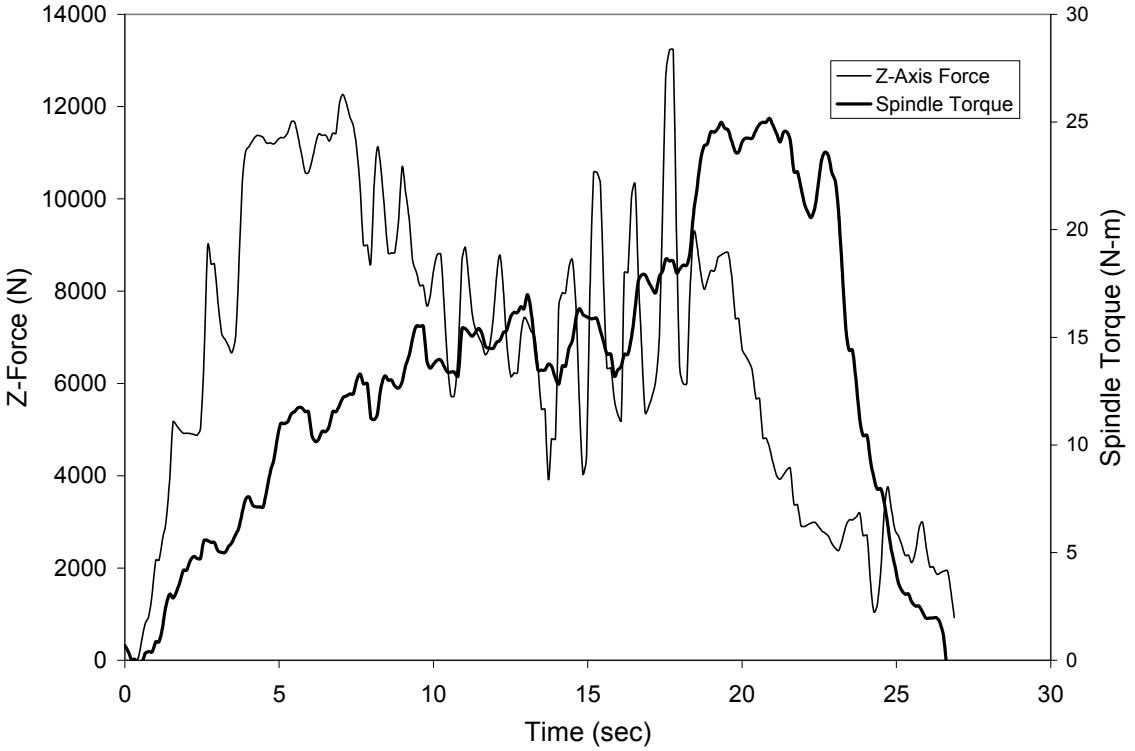

10% Atomic Hydrogen Alloyed CP-Ti

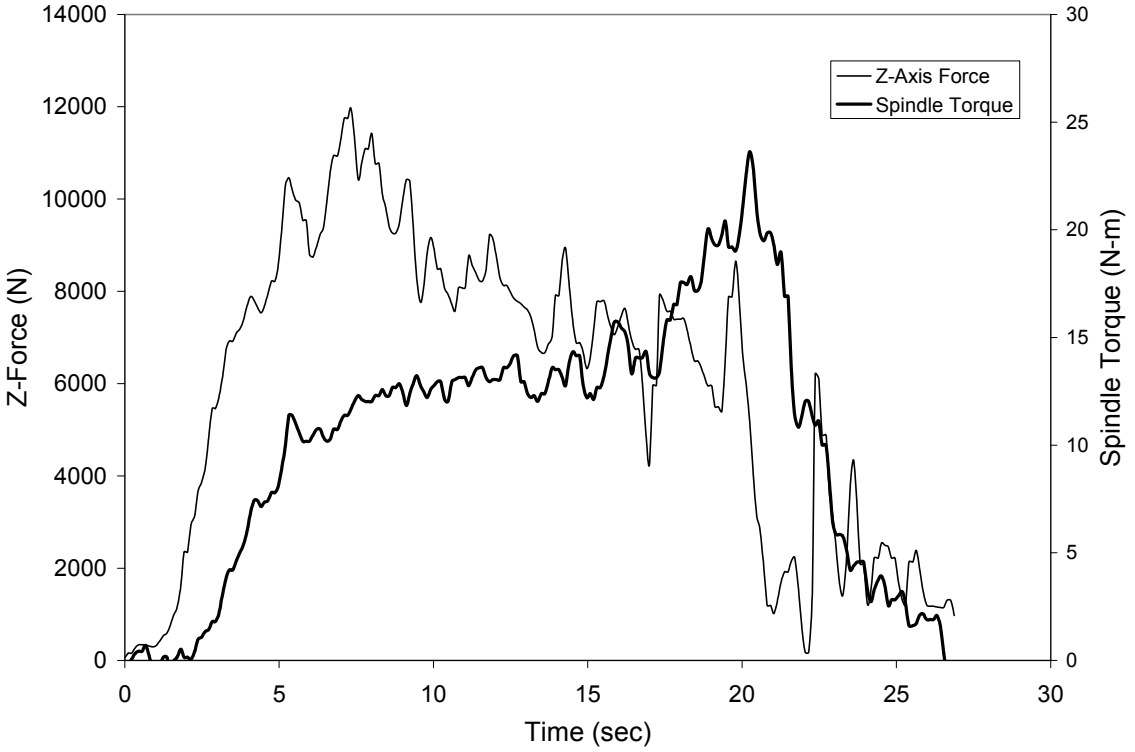

20% Atomic Hydrogen Alloyed CP-Ti

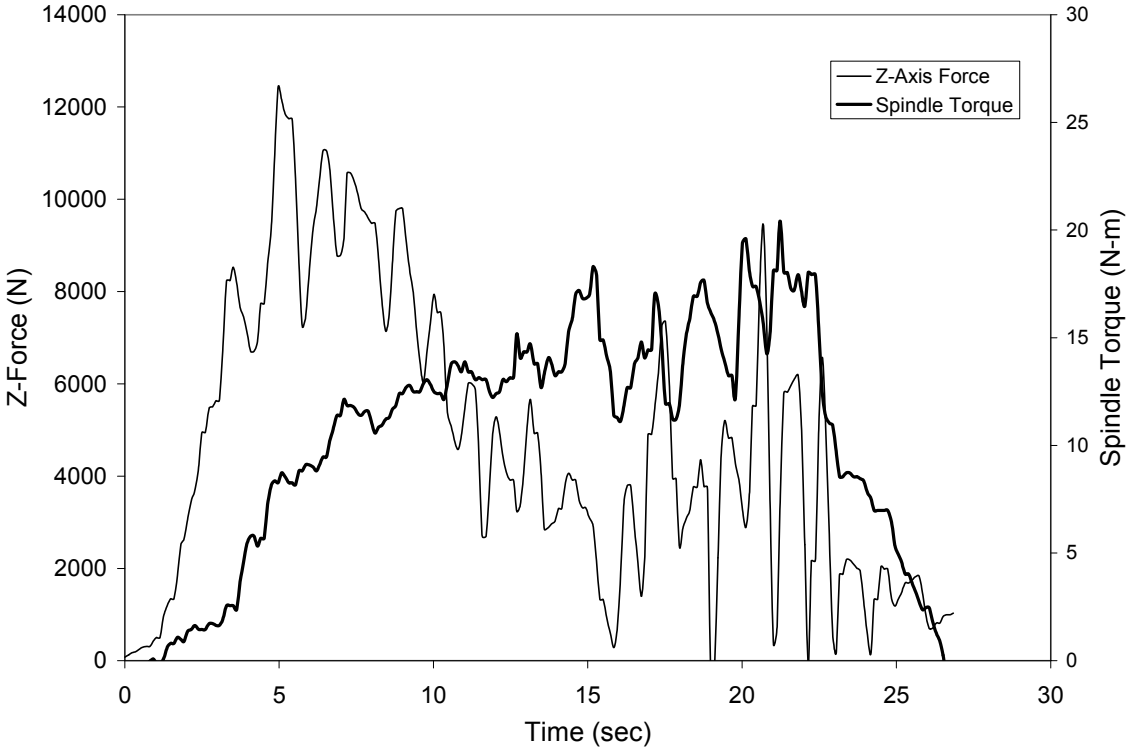

30% Atomic Hydrogen Alloyed CP-Ti